2019

Operational effectiveness of connected vehicle smartphone technology on a signalized corridor

Festo Mjogolo
University of North Florida, n01391515@ospreys.unf.edu

OPERATIONAL EFFECTIVENESS OF CONNECTED VEHICLE SMARTPHONE TECHNOLOGY ON A SIGNALIZED CORRIDOR

By

Festo Mjogolo

A thesis submitted to the School Engineering
In partial fulfillment of the requirements for the degree of
Master of Science in Civil Engineering

UNIVERSITY OF NORTH FLORIDA
COLLEGE OF COMPUTING, ENGINEERING, AND CONSTRUCTION
April 2019

The thesis "Operational Effectiveness of Connected Vehicle Smartphone Technology on a Signalized Corridor" submitted by Festo Mjogolo in partial fulfillment of the requirements for the degree of Master of Science in Civil Engineering has been

Approved by the thesis committee: **Date:**

_______________________________ _________________

Dr. Thobias Sando,
Thesis Advisor and Committee Chairperson

_______________________________ _________________

Dr. Christopher Brown,
Committee Member

_______________________________ _________________

Dr. John Nuszkowski,
Committee Member

Accepted for the School of Engineering:

_______________________________ _________________

Dr. Osama Jadaan,
Director

Accepted for the College of Computing, Engineering, and Construction:

_______________________________ _________________

Dr. William Klostermeyer,
Interim Dean

Accepted for the University of North Florida:

_______________________________ _________________

Dr. John Kantner,
Dean of the Graduate School

DEDICATION

I would like to dedicate this thesis to my God whose Grace has always been sufficient to me.

ACKNOWLEDGEMENTS

I would like to express my sincere gratitude to every person who contributed in one way or another in developing the idea for this thesis. I would like to thank my supervisor, Dr. Thobias Sando, for his unprecedented support, guidance, encouragement and corrective work. His help has been a great support towards the completion of this thesis work.

Special thanks also go to my committee members, Drs. Christopher Brown and John Nuszkowski for their creative ideas and guidance throughout my thesis preparation.

Lastly, I would like to thank all UNF Transportation Laboratory members and my family. I am grateful for everything.

TABLE OF CONTENTS

LIST OF TABLES

LIST OF FIGURES

LIST OF ACRONYMS

ADAS	Advanced Driver Assistance System
API	Application Programming Interface
ASAS	Advance Stop Assist System
CADD	Computer Aided Design and Drafting
CBD	Central Business District
COM	Component Object Model
CS	Connected Signals, Inc.
CV	Connected Vehicles
DOT	Department of Transportation
DSRC	Dedicated Short Range Communication
FDOT	Florida Department of Transportation
FFD	Fractional factorial design
GA	Genetic Algorithm
GLOSA	Green Light Optimized Speed Advisory
GRTDC	Get Ready to Drive Chime
HCM	Highway Capacity Manual
I-SIG	Intelligent Traffic Signal System
ITE	Institute of Transportation Engineers
ITS	Intelligent Transportation System
K-S	Kolmogorov-Smirnov
LOS	Level of Service

MOE	Measure of Effectiveness
NB	North Bound
NBT	North-Bound Through
OBU	On-Board Unit
PET	Probe Enabled Traffic
RBC	Ring Barrier Controller
RLVW	Red Light Violation Warning
RMSNE	Root Mean Square Normalized Error
RSU	Roadside Unit
SPaT	Signal Phasing and Timing
SSGA	Stop Sign Gap Assist
SSVW	Stop Sign Violation Warning
TECO	Tampa Electric Company
THEA	Tampa-Hillsborough Expressway Authority
TMC	Traffic Management Center
TRANSYT-7F	Traffic Network Study Tool, Version 7F
TV	Traditional Vehicles
USDOT	United States Department of Transportation
V2I	Vehicle-to-Infrastructure
V2V	Vehicle-to-Vehicle
V2X	Vehicles to Everything
VAP	Vehicle Actuating Program

VB	Visual Basic
VISSIM	Verkehr In Städten – SIMulationsmodell

ABSTRACT

Various Connected Vehicle (CV) technology applications reported in current literature have the potential to solve challenges that face the transportation sector. Over the last decade, extensive research efforts have been placed on performance evaluation and the benefits of innovative CV applications, and findings indicate that CV technology can effectively mitigate the safety, mobility, and environmental challenges experienced on today's transportation networks. The majority of previous research has evaluated CV technology through simulation studies. However, a field study provides a more ideal method of assessing CV technology effectiveness. Field observational studies to validate previous research findings have not been conducted. Therefore, a field study to obtain the actual effectiveness of CV technology was warranted, not only to validate previous findings, but also to add to the body of knowledge surrounding this topic. This thesis presents both a field study and simulation evaluation of the effectiveness of CV smartphone technology on a signalized corridor. A 1.1 mile segment of State Road 121 (SW 34th Street), containing five intersections, in Gainesville, Florida was selected for study. Field observations were conducted using a fairly new CV application, developed by Connected Signals, Inc., that uses a smartphone application, called EnLighten, to communicate intersection information to driver's smartphone, which serves as a vehicle on-board unit.

Traffic operation and safety performance was evaluated using three measures of effectiveness (MOEs): start-up lost time, discharge distribution model, and speed harmonization. Findings show that the CV smartphone technology improved intersection performance with a reduction in start-up lost time of approximately 86%. Additionally, driving safety improved with a reduction in speed variability by nearly 61% between vehicles in a specific lane for a 100% CV penetration rate. Cost analyses of deploying CV smartphone

technology indicate that implementation may result in an average total economic cost savings associated with crashes of nearly \$6.8 million at the study site, and approximately \$5.6 billion statewide.

Traffic operational effectiveness was also evaluated using a Vissim microscopic simulation approach, based on five MOEs: vehicle travel times, vehicle stop delay, vehicle control delay, queue length, and fuel consumption. Findings revealed that the CV technology improved performance of intersections operating at a Level of Service (LOS) B or better, compared to lower operating levels. Moreover, operational performance increased with an increase in CV penetration rate for intersections with LOS B or better, except for the case where the number of vehicles stop at the approach was less than six per one hundred vehicle-units. Operational performance improved with CV technology at intersections operating at a LOS C with a 30% to 60% CV penetration rate.

Keywords: CV Technology, Smartphone, Start-up Lost Time, Discharge Headway, VISSIM, Genetic Algorithm, Traffic Safety, Connected Vehicles, Vehicle-to-Infrastructure, Microsimulation, Advisory Speed, and Economic Cost Savings.

CHAPTER 1 INTRODUCTION

Background

The innovation of Intelligent Transportation Systems (ITS) has provided the transportation industry with a number of solutions to improve traffic safety and operations, as well as reduce the impact of transportation-related activities to the environment (Jadaan, Zeater, & Abukhalil, 2017). In the early 2000s, the United States Department of Transportation (USDOT) developed the Vehicle-to-Infrastructure Integration program as part of its ITS program (RITA, 2010). The main objective of the program was to promote innovation of intelligent/connected vehicles by introducing vehicle-to-vehicle (V2V) and vehicle-to-infrastructure (V2I) communication platforms to improve traffic safety and mobility (RITA, 2010). As a result, extensive research has been conducted on the performance and benefits of innovative connected vehicle (CV) applications over the last decade, mostly through simulation studies. A study by Njobelo et al. (2018) evaluated the Advanced Stop Assist System (ASAS), which utilizes V2I communication to provide vehicles with advisory speed messages to prevent hard braking events during yellow and all-red signal phases. This microscopic simulation study showed that ASAS could potentially reduce hard braking events by nearly 50% at 100% CV market penetration. To validate these findings, a field study was needed at available sites with CV deployments.

CV technologies have been deployed on various arterial roadways in Florida. These initiatives include the Tampa-Hillsborough Expressway Authority (THEA) Connected Vehicle Pilot, the Gainesville Signal Phase and Timing (SPaT) Trapezium, and the US 90 SPaT deployment in Tallahassee (Florida Department of Transportation [FDOT], 2017) .

The THEA CV pilot project includes various applications, which focus on safety and mobility for multiple travel modes (i.e., streetcars, buses, passenger cars, and pedestrians) in and around downtown Tampa. The deployment approach addresses six use cases: morning backups and congestion, wrong-way entries, pedestrian safety, transit signal priority optimization and safety, Tampa Electric Company (TECO) Line Streetcar conflicts, and enhanced signal coordination and traffic progression (FDOT, 2017). Each case uses at least one CV application. Enhanced signal coordination and traffic progression focus on monitoring peak queuing and congestion using probe enabled traffic (PET) monitoring, and improve traffic progression using the Intelligent Traffic Signal System (I-SIG) (FDOT, 2017).

Florida Department of Transportation (FDOT), in partnership with the City of Tallahassee, implemented SPaT applications on 22 signalized intersections along US 90 (Mahan Drive) in Tallahassee using CV technology (FDOT, 2017). These signalized intersections are equipped with dedicated short-range communication (DSRC), which enable CVs to receive SPaT information through their on-board units (OBUs). This technology is expected to improve intersection safety, and help agencies to gain experience in the operation and maintenance of CV infrastructure and applications (FDOT, 2017).

The City of Gainesville has deployed CV technologies on 27 signals along four corridors forming a trapezium around the University of Florida campus (FDOT, 2017). The goal of this project is to improve travel time reliability, safety, throughput, and traveler information (FDOT, 2017).

Implementation of the aforementioned projects involved the installation of roadside units (RSUs) to broadcast SPaT information to vehicle OBUs for vehicles to be able to receive the SPaT information (FDOT, 2017). Installation of RSUs and vehicle OBUs is expensive, especially OBUs, due to the number of sensors used build and test these project-specific electronic systems (Alves de Lima, 2015). To circumvent the need for installing expensive OBUs to evaluate the study corridor, this study focused on CV technologies that can be used with a smartphone, as an alternative to OBUs. Several of the aforementioned projects, including a number of intersections in Tampa and Gainesville currently employ the CS technology, where a smartphone can be used as an OBU. Using cellular networks, the CS application delivers SPaT information and advisory speeds (within the posted speed limits) directly to a driver's smartphone equipped with the EnLighten application (Connected Signals Inc., 2018).

Study Objectives

Previous research efforts have evaluated the performance and benefits of a variety of CV safety and mobility applications using a simulation approach. However, a field study provides the most ideal method for evaluating CV applications in actual traffic conditions. Therefore, the goal of this thesis was to conduct a comprehensive field test to evaluate the actual performance and benefits of CV technologies in improving safety and mobility at signalized intersections. The study used the CS technology with the EnLighten application since it has already been deployed in various Florida cities. This allowed for the use of a smartphone as an OBU to receive SPaT and advisory speed information to perform the evaluation. The primary objectives of the study included:

1. Evaluate the impact of CV technology on reducing the start-up lost time at a signalized intersection.
2. Evaluate the effectiveness of the CV technology on improving traffic safety.
3. Propose and demonstrate a new methodology for field evaluation of the safety impact of CV technology through speed harmonization.
4. Perform an economic cost savings analysis of deploying CV smartphone technology for the study corridor and statewide.
5. Develop a Vissim driving model of CVs in mixed traffic, based on the field observations.

6. Evaluate the impact of CV smartphone technology deployment on a signalized corridor using a microscopic simulation approach.

Potential Benefits

The majority of previous research evaluated the performance and benefits of a variety of CV applications using a simulation approach. This study evaluated the effectiveness of CV technology under real-world conditions. This thesis work offers potential benefits including, a better understanding of the effectiveness of CV smartphone technology on traffic operations and safety, and the economic cost savings associated with deploying this type of CV technology in terms of crash cost. In addition, this thesis work evaluates the driving behaviors of CVs in mixed traffic conditions, based on the field observations. A microsimulation evaluation of the field data was also conducted to add to the body of knowledge related to CV technology. Furthermore, findings from this research may be useful to transportation agencies when considering future CV deployments.

Thesis Organization

This thesis contains seven chapters. Chapter 1 provides general background information and an overview of the research problem, objectives, and potential study benefits. Chapter 2 gives a brief explanation of the CV technology used in this study, i.e., the CS smartphone CV application. It also discusses the criteria for site selection and a description of the study area, and provides a brief explanation of the methodology used for field data collection. Chapter 3 focuses on the field evaluation of the start-up lost time measure of effectiveness (MOE). Chapter 4 discusses the safety evaluation based on field observations. Chapter 5 discusses the simulation study based on field observations. Chapter 6 summarizes the findings of the evaluations performed, and Chapter 7 outlines the conclusions and recommendations for future work.

CHAPTER 2 METHODOLOGY

Connected Vehicle Application Used

This study used the EnLighten application that enables smartphones to function as OBUs. The EnLighten smartphone application was developed by Connected Signals, Inc., a connected-vehicle data company, which has collaborated with a number of transportation agencies to address the complexities of gathering real-time signal data (Connected Signals Inc., 2018). The decision to use this CV smartphone technology to evaluate SPaT deployments at signalized intersections was based on the following criteria:

- Unlike other connected-vehicle technologies, this approach does not require costly infrastructure investments, such as RSUs.
- This technology uses smartphones, and does not require costly OBUs.
- The CS system communicates with existing traffic-signal infrastructure and translates different manufacturer's signal data to a common format.
- The EnLighten application ensures safety by alerting the drivers to possible dangers without distracting them. For example, the advisory speed alert gives a driver the ability to know in advance whether they can clear the intersection without stopping, or must prepare to stop if a red traffic signal is imminent. The application ensures drivers are not distracted by waiting for a vehicle to come to a complete stop before the visual red countdown is provided.

How The Smartphone Application Works

EnLighten, the smartphone application used in this study, uses sophisticated algorithms that deliver real-time, predictive traffic signal data (Connected Signals Inc., 2018). The Enlighten application provides a driver with information such as advisory speed, visual red light countdown, and a get ready to drive chime (GRTDC). The advisory speed is provided in visual form (an-arc on a speedometer) which advises a driver of the speed required (within posted speed limits) to clear the approaching intersection without stopping. A visual red countdown enables drivers to know the remaining time until a signal turns green. This gives drivers the awareness of how long they will wait for the green light. The GRTDC is an alert sound to tell the driver to focus on the road a few seconds before the light turns green. The system uses cellular networks as a mode of communication.

Site Selection

The process of site selection started with a reconnaissance survey of all sites in Florida that have deployed the CS System. These sites included: Tampa's connected signals in the downtown area, southwest, and along Bruce B Downs Boulevard, and Gainesville's connected signals on Archer Road, Southwest 13th Street, and SW 34th Street (see Figure 2-1). Criteria for site selection included: accurate prediction of upcoming signal states; enough spacing between intersections for speed guidance; at least three lanes in one direction to increase the chance of lane change maneuvers; and high visibility conditions (i.e., free of tall buildings, tree canopy, etc.) to maneuver drones more easily and obtain higher quality aerial video. The solid blue dots shown in the Figure 2-1 maps represent intersections with connected signals, and potential study sites are highlighted in green. From these potential sites, the SW 34th Street (State Road 121) corridor, containing five intersections, in Gainesville, was chosen as the best fit, based on the selection criteria. The geometric characteristics of this corridor were also suitable for evaluating the proposed MOEs.

(a) Downtown and South area in Tampa
(b) Bruce B Downs Blvd Corridor, Tampa
(c) Gainesville Corridors

Note: Blue dots represent intersections with connected signals, Green line is corridor of interest.
Source: ArcGIS Map (not to scale).

Figure 2-1: Corridors with Connected Signals technology in Florida.

Description of the Study Site

The selected study site consisted of a 1.1 mile segment of SW 34th Street (SR121), in Gainesville, Florida. As shown in Figure 2-2, this segment of SR121 is a 6-lane divided roadway five signalized intersections... Three intersections are spaced at approximately 0.25 miles apart, which provides a sufficient distance for drivers to efficiently follow the advisory speed offered by the EnLighten application. The geometric characteristics of this corridor segment are also conducive for evaluating the proposed MOEs. Lane change behavior evaluations require a 4-lane roadway, at a minimum, to increase the number of lanes for performing lane change maneuvers.

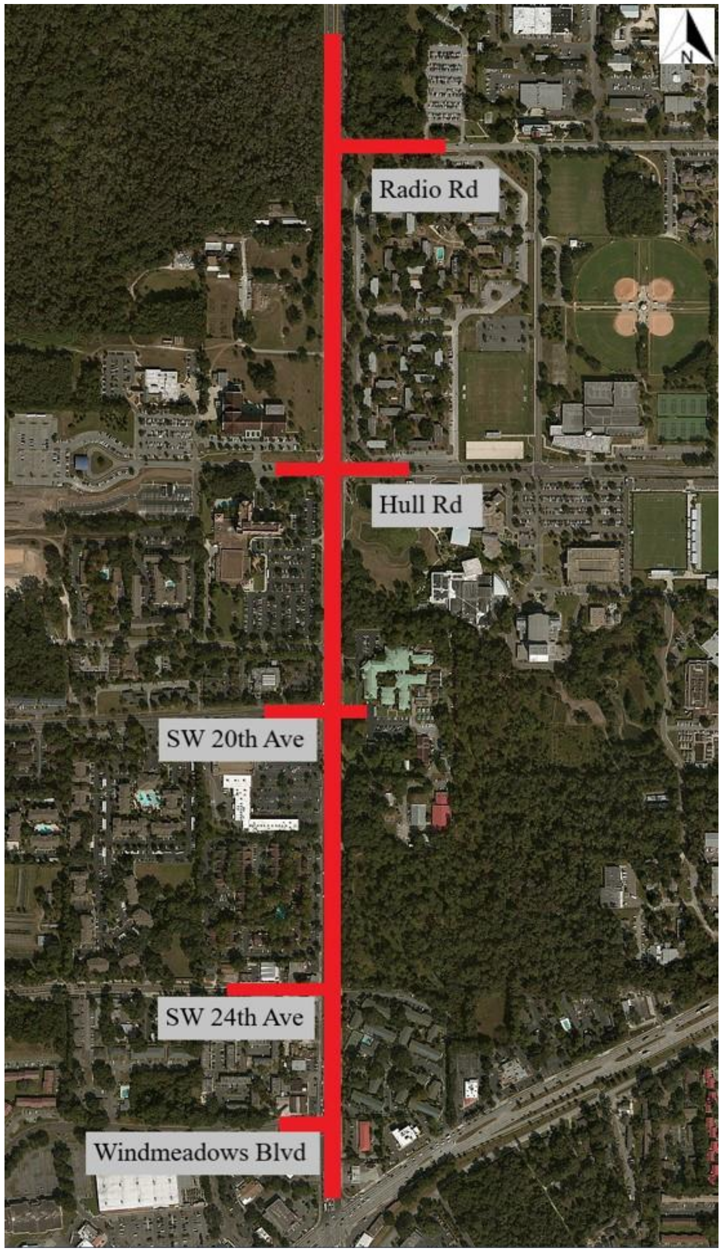

Source: Bing map, 2019 (not to scale)

Figure 2-2: Study site location map.

Data Collection

Data Collection Duration

The data collection exercise aimed at gathering data necessary for evaluating the operational effectiveness of CV technology, specifically for determining the impact of the V2I application on traffic operations and safety. Field data was collected during good weather conditions (sunny days), during daylight hours with dry pavement conditions. To represent typical weekday travel conditions and driver behavior, data were collected on weekdays, Tuesday through Thursday, during the morning and the afternoon off-peak periods, from 10:30am to 12:30pm, and from 1:30pm to 3:30pm, respectively. These time periods were selected for two reasons: first, to increase the chances of a CV study vehicle being the leading vehicle in the standing queue waiting for the next green phase, and second, to increase the CV market penetration rate (i.e., the ratio of CVs to the total number of vehicles in the traffic stream), due to lower traffic volumes during these time periods.

Data Collection Method

Videotaping the intersection is one of the recommended methods for data collection in case of limited manpower (Currin, 2001). Videotaping techniques used in this study included drone video coverage, cameras mounted above ground on signal poles, and ground level cameras mounted on tripods, as shown in Figure 2-3.

(a) Drone camera (b) Top mounted camera (c) Ground level camera

Figure 2-3: Video recording setup.

Lane change behaviors, and the length of standing queues were captured using a drone, since ground level cameras were ineffective in capturing this data due to roadway vertical geometry and mounting height. The drone videos also provided a significantly large amount of vehicle travel time and speed data. Mounted cameras were used for recording vehicle discharge headways at the intersections. The two mounted cameras (top and ground cameras) were used simultaneously for signal change synchronization purposes.

Equipment Used for Data Collection

Equipment used for data collection included:

- 20 cameras with their support tools, including 10 tripod-stands,
- One Drone,
- Smartphones,
- IPad air device,
- Safety gear (i.e., reflective vests and hats),
- Vehicle identifiers (duck tapes), and
- 12 CV equipped vehicles (application-enabled smartphones).

Manpower included drivers and drone crew members. All drivers were civil engineering graduate students from the University of North Florida and University of Florida. Vehicles used were rented for University of North Florida students; however, each student from University of Florida was required to drive his/her own car. Duck-tape with different colors were placed on the tops of each vehicle for CV identification purposes, as shown in Figure 2-4.

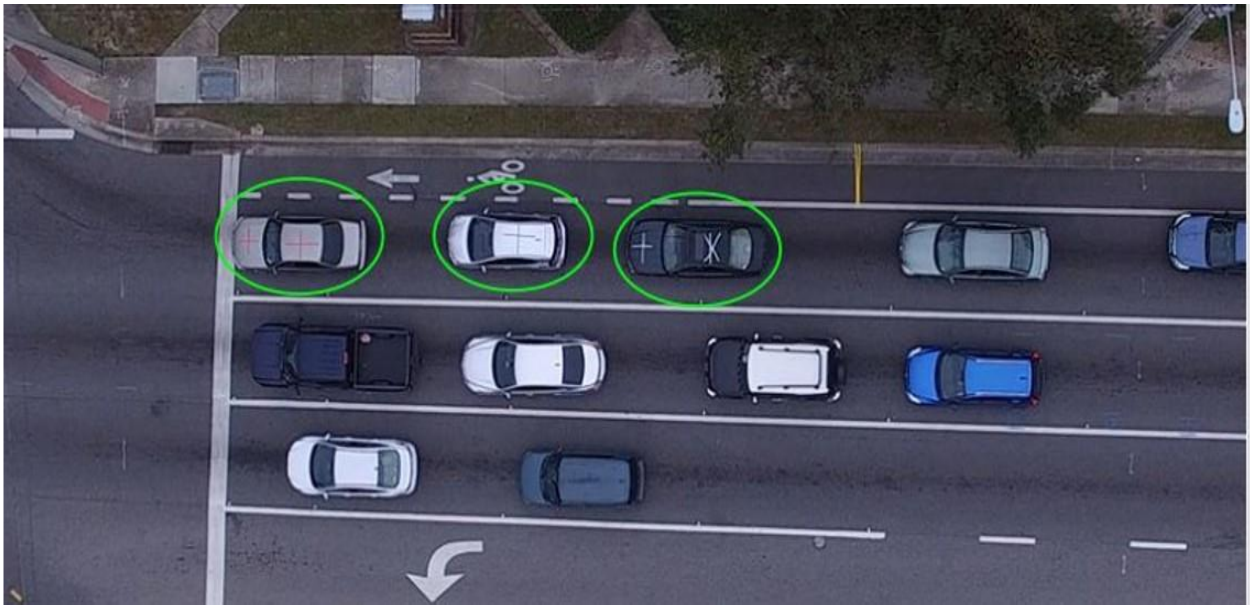

Figure 2-4: A drone picture showing marked connected vehicles used in the study.

CHAPTER 3 TRAFFIC OPERATION EVALUATION: FIELD TEST

Introduction

Much of the travel delay associated with arterial roadways occurs at signalized intersections. A fundamental type of delay experienced at signalized intersections is the start-up lost time. Start-up lost time occurs from a drivers' late response to the change in signal indication (red to green) (Mannering & Washburn, 2014). Late response times further increase if drivers are distracted (Hurwitz et al., 2013). While strategies, such as actuation, coordination, and adaptive controllers reduce start-up lost time, some vehicles will inevitably have to stop on red phases, and stoppage can eventually result in start-up lost time when given a green indication. Recent innovations in CV technology have the potential of helping to reduce start-up lost time, by giving drivers a cue of the change of signal state, thus minimizing the distracted driver component of start-up lost time. Driver cues to the change of signal state is reported to have an impact on the start-up lost time and discharge headways distribution models (Sharma, Vanajakshi, & Rao, 2009).

Various CV applications have been deployed in new vehicles, enabling communication between vehicles (V2V), vehicles to roadside infrastructures (V2I), and vehicles to everything (V2X) (Albertengo et al., 2014). Today's vehicles are gradually becoming more intelligent through the implementation of electronic systems known as ADAS (Advanced Driver Assistance Systems) (Neto, De Lima, & Neto, 2016). ADAS enhance road safety by providing driving assistance in the way of lane keeping assistance, lane changing assistance, collision alert, and adaptive cruise control (Soualmi, Sentouh, Popieul, & Debernard, 2014). However, implementing ADAS is expensive, incorporating a number of sensors, and often propriety electronic systems (Alves de Lima, 2015).

Integration of cloud computing on smartphones provides a platform to implement smart vehicle applications of nearly similar capabilities to ADAS (Neto et al., 2016). Smartphones are widely used in society, making it more affordable and scalable option. Vehicle crash detection by estimating the gravity-force on the passengers, driver's sleepiness detection application, and TrafficCam are smart vehicle applications that have been implemented (Calafate et al., 2011; Fattah et al., 2015).

Objectives

To evaluate the benefits of the CV smartphone technology, two objectives were established. The first objective was to examine whether implementing the CS technology could reduce start-up lost time at signalized intersections. The second objective was to evaluate the impact of CV smartphone technology on discharge headway distribution. Findings may potentially assist traffic engineers in adjusting capacity estimation to account for CV technology adoption when performing traffic operational analyses.

The Chapter is organized as follows:

- Literature on start-up lost time, the distribution model of discharge headways, and CV Smartphone Technology and distracted drivers is discussed,
- The evaluation methodology is presented, including the equipment used, equipment setup techniques used, and video data extraction,
- MOE results and the statistical method used to test their level of significance are presented, and
- Lastly, a discussion of the results is presented.

Literature Review

Start-up Lost Time

Start-up lost time has been reported to range from one to two seconds (National Research Council U.S. Transportation Research Board, 2010). Several studies, however, have found start-up lost time falling outside this typical observed range, with a minimum of 0.75 seconds and a maximum of 3.04 seconds (Cartens, 1971; J. Lee & Chen, 1986). These studies found that start-up lost time is caused by an additional time (in seconds) consumed by the first four or five vehicles in a queue (Hurwitz et al., 2013). According to the Institute of Transportation Engineers (ITE) data collection manual, only the first four vehicles are used to determine the start-up lost times (Currin, 2001). Therefore, many studies have calculated the start-up lost time by considering the initial departure headways for the first four to five vehicles (Hurwitz et al., 2013).

Based on literature, there are three different ways of measuring saturation headways in the field. The first method involves measuring time headways of the 4th through 12th vehicle in a standing queue (H. Li & Prevedouros, 2002). The second method considers all the vehicles in the standing queue, regardless of the queue length (National Research Council U.S. Transportation Research Board, 2010; H. Li & Prevedouros, 2002). The last method involves all vehicles in the standing queue, plus arrival vehicles that join the standing queue, as long as the arriving vehicles were within 140 feet from the stop line (H. Li & Prevedouros, 2002).

Factors Affecting Start-up Lost Time

Factors that affect the start-up lost time include intersection location (e.g., Central Business District (CBD) or non-CBD), signal phase sequencing, leading/lagging left turn signal phase, intersection geometry (i.e., number of through lanes, and left turn lanes), grade, percentage of truck volume, weather conditions, queue length, visibility of traffic light, and drivers' state of driving (Shawky & Al-ghafli, 2016).

A study by Bonneson, (1992) found that the left-turn radius affects start-up lost time. Al-Ghamdi (1999) investigated the effect of number of lanes on the average discharge headway for through movements at urban signalized intersections. The results indicated that start-up lost time for two lanes is significantly higher than that of three lanes (Al-Ghamdi, 1999). Shawky and Al-ghafli (2016) found that intersection location, phase split, and lead/lag phasing have significant impact on the start-up lost time. However, the study did not find significant differences between peak and off peak periods (Shawky & Al-ghafli, 2016). Li and Prevedouros (2002) conducted detailed observations of saturation headways and start-up lost times. Results showed that the left-turning movement had shorter start-up response time than the through movement, and the estimated start-up lost times were higher than those shown in the Highway Capacity Manual (HCM) (H. Li & Prevedouros, 2002). The study also showed that the magnitude of queue length affects the field measurement of the saturation flow rate for both through and left-turning protected vehicles.

Distribution Model for the Start-up Lost Time

An appropriate distribution model is essential for accurate estimation of traffic measures, such as vehicle delay and start-up lost time (Tan, Li, Li, & Zhang, 2013). Researchers have investigated appropriate distribution models for the start-up lost time by considering their relations with departure headway distributions. The distribution model of discharged headways of each position of the vehicle in a queue was found to follow a certain log-normal distribution (Jin et al., 2009). However, Yin et al. (2011) proposed that departure headways approximately follow position-dependent log-normal distributions, with the exception of the first queued vehicles (Yin et al., 2011). Tan et al. (2013) proposed a distribution model for start-up lost time, in that the first four departure headways follow log-normal distributions. The best fit distribution of the field collected discharge headways during off peak hours was observed to be a log-normal distribution (Zhang, Wang, Wei, & Chen, 2007).

CV Smartphone Technology and Distracted Drivers

Distracted driving may occur if a driver is sleepy or drowsy, or engaging in other secondary tasks, such as using a mobile device, while driving (Bej, Rakshit, Mal, & Mahapatra, 2019). Mobile phone activities with high visual demands, such as texting and browsing, increase the chance of collision during driving (X. Li, Oviedo-Trespalacios, Rakotonirainy, & Yan, 2019). Mobile devices require a multitude of cognitive and physical resources that distract drivers, resulting in poor driving performance (Oviedo-Trespalacios, King, Haque, & Washington, 2017). Understandably, CV technology that utilizes smartphones as OBUs may increase the risk of driver distraction, due to the visual demands to register some of the provided information, such as the visual red signal countdown. However, the EnLighten application is designed in such a way that ensures drivers are not distracted while using it. This is ensured by waiting for a vehicle to come to a complete stop before the visual red countdown is provided. The application also turns off all other visual information and provides only audio notifications when the phone placed in the horizontal position.

Methodology

Field Evaluation of Start-up Lost Time

Start-up lost time was evaluated from the vehicle discharge headways obtained from video data recorded in the field. Different camera setups were deployed to facilitate accurate discharge headway data collection. The camera setup deployed consisted of:

1. A top camera mounted on a traffic signal post.

   This camera setup was used specifically to determine the time at which the front bumper of the vehicle crosses the stop line. Traffic Management Center (TMC) cameras and mounted cameras were used for this purpose.

2. A ground camera.

   This camera was used for synchronization purposes to coordinate with the video recorded by the top camera to determine the exact time at which the signal changed from red to green in order to accurately determine the discharge headway of the first queued vehicle.

3. Drone for aerial view.

   The drone was used to capture the extent of the standing queue, so that only discharge headways from the stopped vehicle were recorded. This method is discussed in the ITE data collection manual, which recommends that only discharge headways of the standing queue should be used for evaluating saturation flow (Currin, 2001).

For the purpose of evaluating the operational effectiveness of CV smartphone technology on startup lost time, CV trained drivers were encouraged to drive in groups of at least four vehicles per lane and focus on utilizing the "get ready to drive chime" (GRTDC) information. Based on literature, discharge headways of at least the first four vehicles are involved in the determination of start-up lost time; therefore, drivers were encouraged to drive in groups of at least four vehicles.

Video Data Extraction

In this study, discharge headways of the through vehicles in a standing queue were measured from the recorded video data. Therefore, a standing queue and a through lane were the two criteria used in the video data extraction process for evaluating the start-up lost time. Figure 3-1 shows a flowchart of the steps used to determine the start-up lost time for both conventional vehicles, referred to as traditional vehicles (TVs) in this study, and CVs.

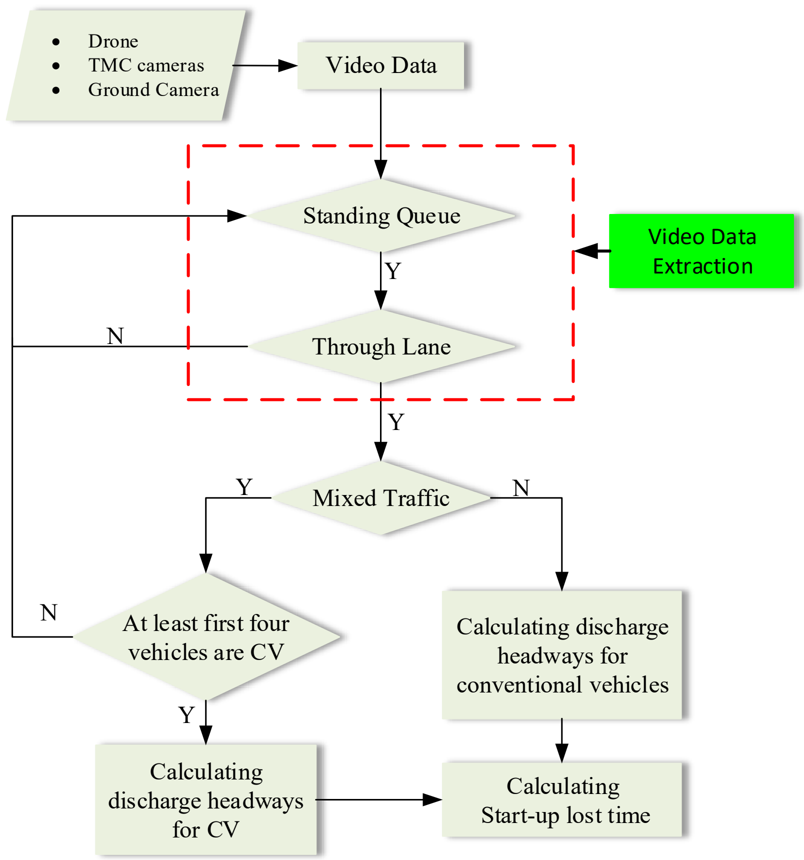

Figure 3-1: Flow chart for determining start-up lost time for both TVs and CVs.

Data Analysis

Discharge Headways

The analysis considered two categories of vehicles – TVs and CVs. TVs refer to vehicles that do not have communication with roadside infrastructure. At least 67 cycles were evaluated, more than the minimum 15 cycle lengths with at least 8 queued vehicles generally recommended for a field evaluation of saturation flow rate and start-up lost time (Currin, 2001)). Discharge headways were recorded using a video timer with an accuracy of 0.01 seconds. Tables 3-1 and 3-2 show the statistical summary of the observed discharge headways for the two categories, TVs and CVs, respectively. The mean discharge headways for the two categories are graphically represented in Figures 3-2 and 3-3.

Table 3-1: Statistical Parameters of Traditional Vehicle Discharge Headway

P	N	Mean [sec]	Max [sec]	Min [sec]	Mode [sec]	Median [sec]	SD [sec]	Skewness
1	178	2.71	4.79	1.22	2.66	2.66	0.836	0.439
2	186	3.37	4.64	2.08	3.61	3.37	0.617	-0.143
3	183	2.51	4.43	1.41	2.04	2.35	0.640	0.785
4	174	2.38	5.86	1.55	2.82	2.34	0.677	2.638
5	143	2.39	4.32	1.07	2.84	2.31	0.709	0.588
6	117	2.26	5.97	1.02	1.46	2.15	0.873	1.770
7	103	2.25	3.37	1.16	2.17	2.25	0.596	0.063
8	82	2.26	5.72	1.01	1.6	1.96	0.954	1.892
9	76	2.41	4.41	1.17	1.86	2.39	0.805	0.715
10	67	2.10	5.2	1.05	1.61	1.94	0.793	2.146

Note: P = Position in the queue, N = Number of observed vehicles, Max = Maximum, Min = Minimum, SD = Standard deviation, Sec = Seconds.

Table 3-2: Statistical Parameters of Connected Vehicle Discharge Headway in Mixed Traffic

P	N	Mean [sec]	Max [sec]	Min [sec]	Mode [sec]	Median [sec]	Skewness
1	134	1.04	2	0.25	0.775	0.572	0.586
2	127	2.16	2.9	1.23	2.23	0.407	-0.252
3	107	2.14	3.03	1.46	2.08	0.524	0.663
4	113	2.06	2.82	1.37	1.87	0.431	0.249
5	87	2.07	2.26	1.92	2.02	0.175	1.116
6	67	2.04	2.13	1.96	2.03	0.537	0.987

Note: P = Position in the queue, N = Number of observed vehicles, Max = Maximum, Min = Minimum, SD = Standard deviation, Sec = Seconds.

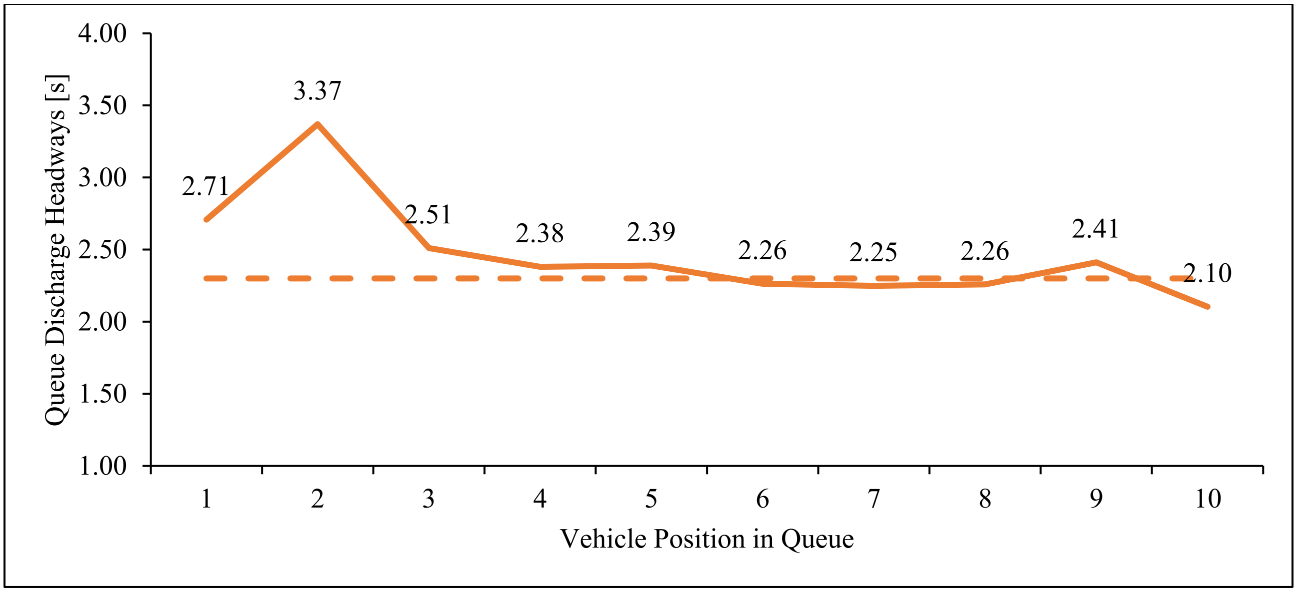

Figure 3-2: Mean discharge headway of traditional vehicles.

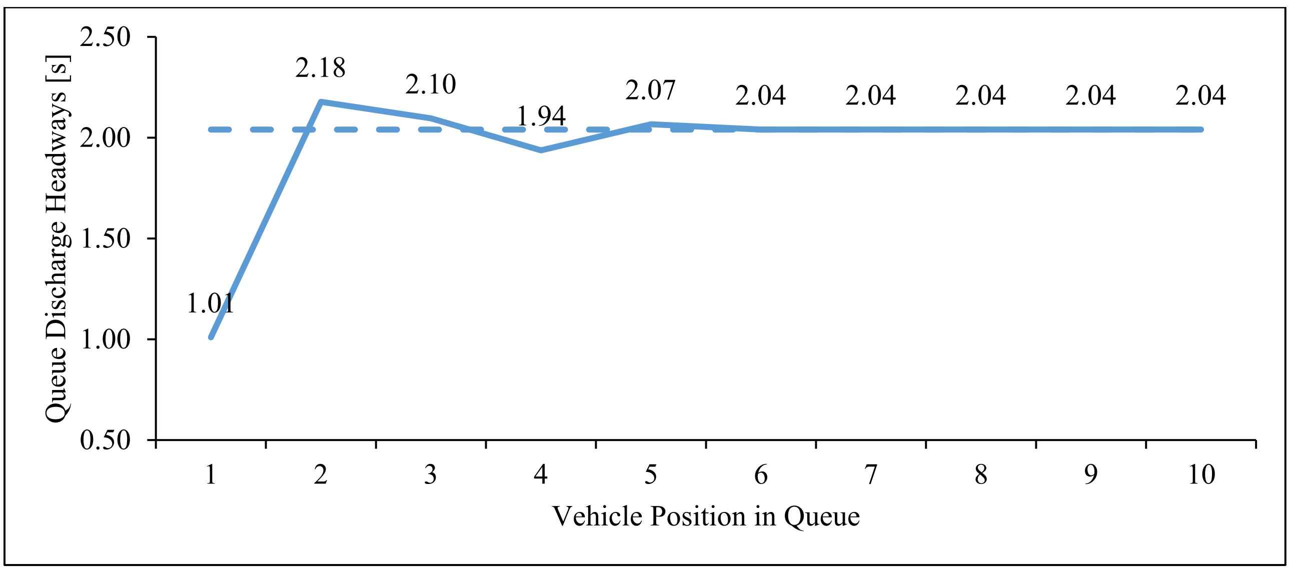

Figure 3-3: Mean discharge headway of connected vehicles in the mixed traffic.

Field Start-up Lost time Estimation

The HCM considers the first four vehicles in a standing queue in estimating the start-up lost time, and the estimation of the saturation headway starts with the fifth queued vehicle (National

Research Council (U.S.) Transportation Research Board., 2010). The start-up lost time was calculated using Equation 3-1.

$$\text{Start} - \text{up lost time} = \sum_{n=1}^{n_4}(\Delta t_n) \qquad \text{Equation 3-1}$$

Where, n= position of the vehicle from the standing queue

Δt_n= difference in discharge headway of each vehicle and the saturation headway

Therefore, based on the average discharge headways, from Table 3-1 and 3-2, the start-up lost times were calculated to be 1.93 seconds and 0.27 seconds for TVs and CVs, respectively.

Fitting of Discharge Headway Distributions in the Connected Vehicle Environment

Knowing the correct distribution model of the discharge headways helps in traffic signal timing, analysis of intersection capacity, and in understanding of driving behaviors (Jin et al., 2009). Therefore, evaluating the impact of the CV smartphone technology on the distribution of the discharge headways is important. Based on previous studies, the distribution of the discharge headways for each vehicle queue position follow a certain position-dependent log-normal distribution despite having different means and variances (Jin et al., 2009). The presence of phase countdown is known to affect discharge headways (Sharma et al., 2009). Therefore, deploying CV technology, especially the V2I component, may have an impact on the discharge headway distribution model, since a driver may respond more quickly to the signal changes because of the cue received from the smartphone application. The CV smartphone technology predicts the upcoming signal phases, thus enabling drivers to focus on the driving task with fewer distractions, especially a few seconds before the signal changes to green.

The Anderson-Darling test (AD) (Stephens, 1974) was used to determine the best distribution that fits the data collected in the field. As opposed to the goodness-of-fit test used by Jin et al., (2009), the Anderson-Darling test was selected because it is a modification of the

Kolmogorov-Smirnov (K-S) test, and gives more weight to the tails than the K-S test. The limitation of the K-S test is that it is distribution free in the sense that the critical values do not depend on the specific distribution being tested. On the other hand, the Anderson-Darling test makes use of the specific distribution in calculating critical values, and it has the advantage of allowing for a more sensitive test.

The Anderson-Darling test was performed under 95% confidence level with the null hypothesis that the discharge headways at each position of the vehicle in the queue follow a certain specific distribution. This null hypothesis was tested against an alternative hypothesis that the discharge headways at each position of the vehicle in the queue do not follow a specific distribution under test. The null hypothesis would be rejected if the resulting P-value was less than 0.05.

The following fifteen (15) parametric distribution models were tested: Normal, Box-Cox Transformation, Log-normal, 3-Parameter Log-normal, Exponential, 2-parameter Exponential, Weibull, 3-Parameter Weibull, Smallest Extreme Value, Largest Extreme Value, Gamma, 3-Parameter Gamma, Logistic, Log-logistic, and 3-Parameter Log-logistic.

The first four discharge headways were taken into consideration because the discharge headways of these vehicles contribute to the start-up lost time. The best distribution was determined by checking the P-value and the Anderson Darling value. The best distribution was the one with a P-value greater than 0.05 and the smallest Anderson-Darling value. Both descriptive statistics and the Anderson-Darling goodness-of-fit test results are summarized in Tables 3-3 and 3-4, respectively, for the first four queued CVs. According to the results shown in Tables 3-3 and 3-4, the best discharge headway distribution of each position, for the first four positions, follow the log-normal distribution, similar to findings obtained by Tan et al. (2013). The Log-normal distribution model is presented in Equation 3-2.

$$f(h) = \frac{1}{\sqrt{2\pi\sigma^2 h}} \exp\left[-\frac{(\ln - \mu)^2}{2\sigma^2}\right], h > 0 \qquad \text{Equation 3-2}$$

Where, μ and σ are model parameters, and h is the discharge headway.

Table 3-3: Descriptive Statistics of the First Four CV Discharge Headways

Position In Queue	N	Mean [sec]	Stdev [sec]	Median [sec]	Minimum [sec]	Maximum [sec]	Skewness	Kurtosis
1	134	1.043	0.572	0.79	0.25	2	0.430	-1.262
2	127	2.163	0.407	2.2	1.23	2.9	-0.148	0.400
3	107	2.140	0.524	2.1	1.46	3.03	0.534	-0.901
4	113	2.064	0.431	1.9	1.37	2.82	0.330	-0.948

Table 3-4: Goodness-of-Fit Test Results of CV Discharge Headway Distributions

Position In The Queue	**1**		**2**		**3**		**4**	
Distribution Name	**AD**	**P**	**AD**	**P**	**AD**	**P**	**AD**	**P**
Normal	0.664	0.07	0.23	0.775	0.56	0.127	0.39	0.347
Box-Cox Transformation	0.391	0.346	0.23	0.775	0.382	0.455	0.306	0.534
Log-normal	0.391	0.346	0.336	0.47	0.379	0.369	0.306	0.534
3-Parameter Log-normal	0.437	*	0.231	*	0.352	*	0.318	*
Exponential	1.857	0.011	5.905	<0.003	5.178	<0.003	5.592	<0.003
2-Parameter Exponential	0.813	0.115	3.122	<0.010	0.516	>0.250	1.358	0.02
Weibull	0.503	0.202	0.286	>0.250	0.633	0.089	0.452	>0.250
3-Parameter Weibull	0.406	0.376	0.257	>0.500	0.336	>0.500	0.29	>0.500
Smallest Extreme Value	0.846	0.024	0.449	>0.250	0.931	0.016	0.614	0.098
Largest Extreme Value	0.555	0.152	0.519	0.186	0.393	>0.250	0.306	>0.250
Gamma	0.463	>0.250	0.273	>0.250	0.459	>0.250	0.356	>0.250
3-Parameter Gamma	0.574	*	4.999	*	0.354	*	0.398	*
Logistic	0.688	0.041	0.248	>0.250	0.525	0.134	0.431	0.238
Log-logistic	0.447	0.221	0.215	>0.250	0.394	>0.250	0.365	>0.250
3-Parameter Log-logistic	0.428	*	0.218	*	0.371	*	0.335	*

Comparison of TV and CV Discharge Headway Distributions

Figure 3-4 shows the comparison between TV and CV discharge headways distribution for each of the vehicle's position in the queue. Results reveal a shift between TV and CV mean discharge headways, and the shift decreases as the queue position increases. These shifts indicate the intersection operation improvement in reducing start-up lost times. There was a shift of 62%, 36%, 15%, and 13% for the first through the fourth queued position, as depicted in Figure 3-5.

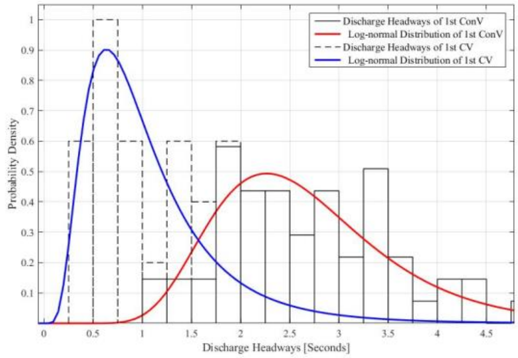

a: Comparison of discharge headway distributions of the first queued vehicle for both TV and CV.

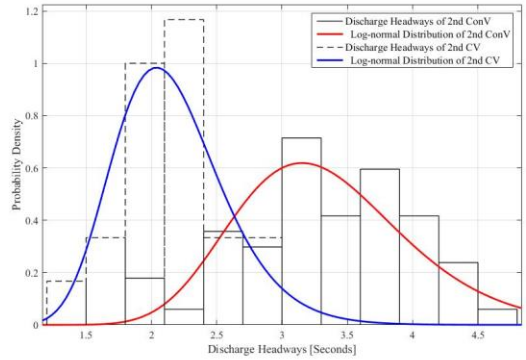

b: Comparison of discharge headway distributions of the second queued vehicle for both TV and CV.

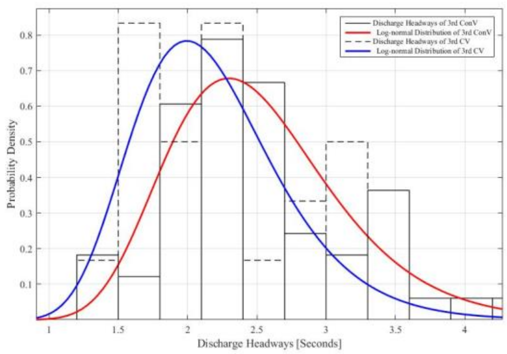

c: Comparison of discharge headway distributions of the third queued vehicle for both TV and CV.

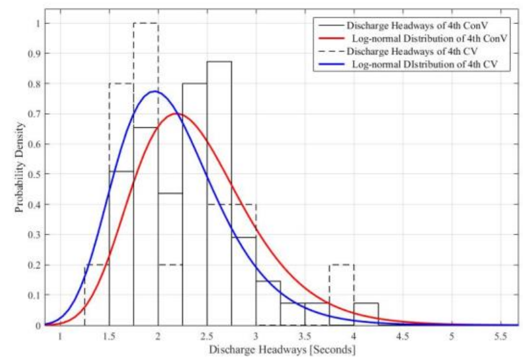

d: Comparison of discharge headway distributions of the fourth queued vehicle for both TV and CV.

Figure 3-4: Discharge headway distribution comparison: first four queued TVs and CVs.

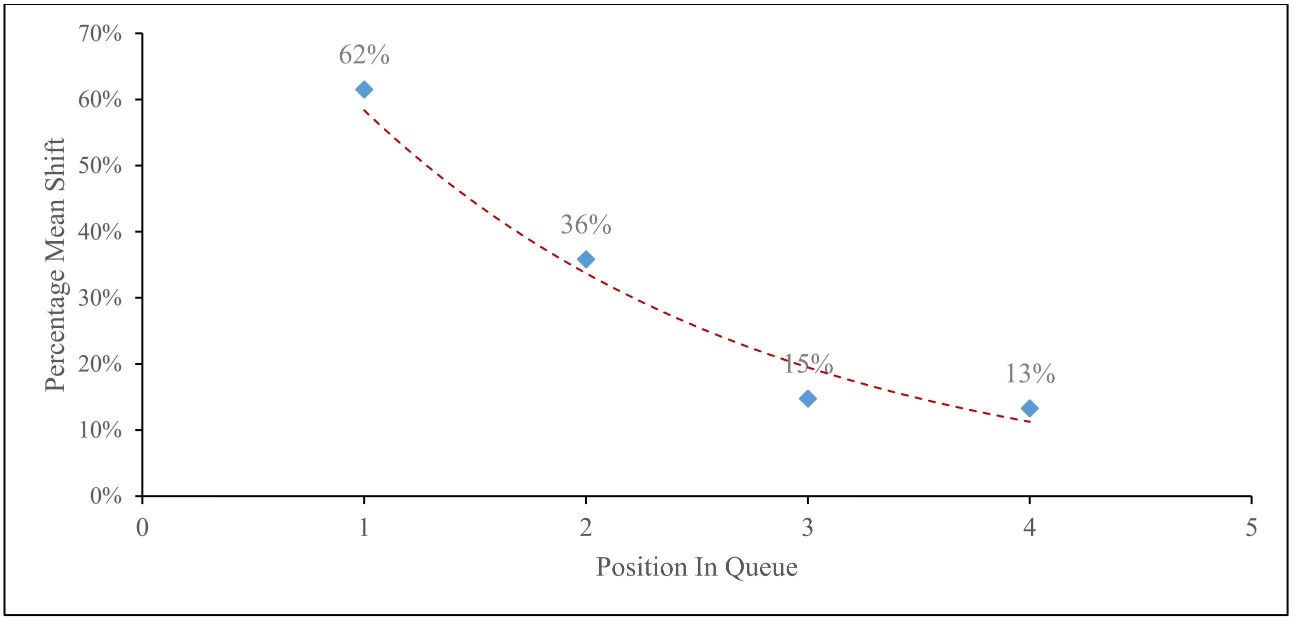

Figure 3-5: Mean shift between TV and CV position-dependent discharge distribution.

Statistical Analysis of Measures of Effectiveness

The Paired T-test was used to evaluate whether CV smartphone technology had a significant impact on the start-up lost time. Since the discharge headways of the first four queued vehicles contribute to the start-up lost time, the mean difference between each of the first four discharge headways of TVs and CVs were statistically compared using the Paired T-test method.

A paired t-test is a statistical procedure used to determine whether the mean difference of two sets of observations is zero. The t-test is applied to the dataset that are normally distributed, therefore, the Anderson Darling goodness-of-fit test was conducted and the results showed that the data sets were normally distributed. Table 3-5 summarizes the Anderson Darling goodness-of-fit test of each of the first four discharge headway datasets, where, normal distribution was among the distributions followed by these datasets.

In the paired t-test, the null hypothesis tested was that the mean differences between the discharge headways of the first four TV and CV queued vehicles is zero. This null hypothesis was tested against the alternate hypothesis that mean differences between the discharge headways of the first four queued TV and CV vehicles is greater than zero as follows.

Null hypothesis: H_0: μ_difference = 0

Alternative hypothesis: H_1: μ_difference > 0

Where: μ_difference = difference between TV mean discharge headway and CV mean discharge headway

The results of the estimation from the paired difference of position-dependent discharge headways are summarized in Table 3-5. According to data shown in Table 3-5, the mean difference of the first four discharged headways between TVs and CVs were significant (P-value < 0.05). Hence, the data suggests that the CV technology reduces the start-up loss time.

Table 3-5: Paired T-Test Results of the Position-Dependent TV and CV Discharge Headways

Estimation for Paired Difference						
H	**μ_d [sec]**	**SD [sec]**	**SE [sec]**	**95% LB [sec]**	**T-Value**	**P-Value**
H1	1.857	0.689	0.167	1.565	11.11	0.000
H2	1.119	0.694	0.168	0.825	6.65	0.000
H3	0.58	0.878	0.213	0.208	2.72	0.008
H4	0.702	1.128	0.274	0.224	2.57	0.010

Note: H = discharge headway, μ_d = Mean difference, SD = Standard deviation, Sec = Seconds, SE= Mean Standard Error, 95% LB = 95% Lower Bound for μ_difference, H1=the number after letter H stands for vehicle position in queue.

Discussion of Results

The Discharge Headway of the Second Standing Queued Vehicle

From the summary of statistics for discharge headways presented in Tables 3-1 and 3-2, an interesting finding for the headways of the second TV and CV vehicle in the queue is noticeable. The discharge headway distribution of the second queued vehicle is negatively skewed, while the discharge headway distributions of all other vehicle positions have a positive skew (see Tables 3-1 and 3-2). This implies that a large proportion of second queued vehicles have discharge headways greater than the resulting mean discharge headways. Therefore, the second queued vehicle seemed to have the largest discharge headway among the other first four queued vehicles, regardless of vehicle type (i.e., TV or CV), as shown in Figures 3-2 and 3-4. Similar results were observed by Yang (2013), Greenshields, Schapiro, & Ericksen (1946), and Krcal, Nagy, & Jerabek (2009). This finding is termed as the second vehicle delay phenomenon, which contradicts intuition that would suggest smaller headways for the second queued vehicles compared to the first vehicles in the queue.

Distribution of the Start-up Lost Time in the Connected Vehicle Environment

An accurate distribution model of the discharge headways is essential in transportation planning and traffic operations analyses, such as intersection capacity analyses and understanding driving behavior at signalized intersections. Due to its importance, this study evaluated the impact of the CV smartphone technology on the distribution of the position-dependent discharge. The results of the Anderson-Darling goodness-of-fit test showed that the best fit distribution of the first four discharge headways is the log-normal distribution (see Table 3-3). This finding is consistent with results reported by previous studies that observed the log-normal distribution to be the best fit for field discharge headways collected during off-peak hours (Zhang et al., 2007; Jin et al., 2009; Tan et al., 2013).

Impact of CV Smartphone Technology on Start-up Lost Time

Studies show that the start-up lost time is caused by the first few vehicles in the standing queue having to react to the initiation of the green phase and accelerate from a stopped position. Literature has suggested measures that could possibly reduce the start-up lost time, such as the use of signal countdown timers (Limanond, Chookerd, & Roubtonglang, 2009; Limanond, Prabjabok, & Tippayawong, 2010; Liu, Yu, Wang, Ma, & Wang, 2012). CV technology enables vehicles to communicate with other vehicles, roadside infrastructure, and with everything related, and is expected to reduce start-up lost time by enabling drivers to react more quickly to changing signal states. Likewise, it was anticipated that the CV smartphone technology analyzed in this study would also indicate an improvement in reduced start-up lost time.

Data collected from the field revealed average start-up lost times of 1.93 seconds and 0.27 seconds for TVs and CVs, respectively. This is equivalent to an 86% reduction in average start-up lost time for CV enabled vehicles. The impact of CV smartphone technology on start-up lost time was also revealed from the comparison between TV and CV position-dependent discharge headway distributions. Results indicated a shift between the mean CV and TV position-dependent discharge headway distributions, which decreases as the vehicle position in the queue increases. The shift represents a reduction in the average discharge headway of CVs compared to TVs. There was a reduction in average discharge headway of 62%, 36%, 15%, and 13% for the first through the fourth queue position, respectively.

CHAPTER 4 TRAFFIC SAFETY EVALUATION: FIELD TEST

Introduction

Travel speed variability at a signalized intersection is one of the factors that contribute to crash occurrences (Bhuiyan, Parentela, & Inapuri, 2016). Over 2.8 million intersection related crashes occur each year in the United States, which account for over 40% of all reported traffic crashes (Bhuiyan et al., 2016). Rapid advancement in CV technology has made continuous real-time traffic monitoring and communication with drivers possible (Dowling et al., 2016). As a result, a variety of traffic safety applications have been developed and implemented (Talebpour, Mahmassani, & Hamdar, 2013). The CS system offers one CV application that utilizes vehicle-to-infrastructure (V2I) communication. This smartphone-based CV application provides drivers with accurate real-time, predictive information about upcoming signal phases as they approach an intersection and offers speed guidance to assist the driver in getting through the intersection without stopping (Connected-Signal, 2018). Real-time speed guidance, in the form of speed advisory messages, promotes speed harmonization to improve driving safety (Connected-Signal, 2018; Dowling et al., 2016). Speed harmonization is an active traffic management strategy that is used not only for improving traffic safety, but also to reduce congestion, maximize traffic throughput, reduce vehicle delay, increase travel time reliability, and reduce the amount of stop-and-go traffic (Talebpour et al., 2013). Developing and implementing speed harmonization methodologies in the connected vehicle environment would enable transportation agencies to gain experience on effective ways of promoting safer driving.

There are limited studies on speed harmonization with CV technology. One study used a microscopic simulation approach to develop and test the on-board advisory system that gives advisory messages on lane, speed, and headway selection (Schakel & Van Arem, 2014). The system optimized lane distribution in high flow conditions, decreased the chance of spillback, and minimized the reduction in capacity drop. Results showed a 49 % reduction in travel time delay (Schakel & van Arem, 2014). Another study developed a Connected Vehicles Harmonizer (CVH) that sends optimal advisory speeds to CVs in work zones (Ramezani & Benekohal, 2015). The system showed a more than 13% delay reduction at the CV market penetration rate of at least 80% (Ramezani & Benekohal, 2015). A microscopic simulation approach was also used to detect shockwaves from breakdown formation and driving hazards, and implemented speed harmonization as a control strategy under congested traffic conditions (Talebpour et al., 2013). Results from the study revealed an existence of an optimal location at an upstream point of shockwave detection to implement speed limit changes and recommend the importance of speed limit compliance for the success of a speed harmonization system (Talebpour et al., 2013). An evaluation of the impacts of CV technology on the effectiveness of variable speed limits on a freeway bottleneck section was conducted by Joyoung Lee & Park (2013) using a microscopic simulation approach.

The aforementioned studies used a simulation approach to examine the impacts of CV technology on speed harmonization. In addition, these studies also addressed the operational effectiveness of speed harmonization using CV technology, such as reducing congestion, maximizing traffic throughput, reducing vehicle delay, increasing travel time reliability, and reducing the amount of stop-and-go traffic. However, none of the studies reviewed in literature conducted a field evaluation of CV technology on these traffic measures. Therefore, there is a need to conduct a field test to evaluate the potential of the CV technology on speed harmonization, and quantify its impact on improving driving safety.

Study Objectives

This study aimed to conduct a field test and propose a methodology to evaluate the potential of CV technology on improving driving safety through speed harmonization. The effectiveness of speed harmonization was evaluated using a smartphone-enabled CV application, called EnLighten, developed by Connected Signals, Inc., that offers an intersection-focused V2I safety application. Findings from the field test evaluation were used to quantify the safety impacts of CV smartphone technology on speed harmonization for various CV penetration rates.

Literature Review

Connected Vehicle Intersection-Focused V2I Safety Applications

Various CV intersection-focused VI2 safety applications have been developed to enhance both traffic and pedestrian safety. The Red Light Violation Warning (RLVW) V2I safety application uses the position of the intersection and the speed of the vehicle to send SPaT and other data to an in-vehicle device that advises drivers of an upcoming signalized intersection and provides a warning to prevent the driver from violating a red light (Stephens, Schroeder, Klein, & Institute, 2015). RLVW can also be used at a railroad crossing to help minimize violations related to railroad crossing gates.

The Green Light Optimized Speed Advisory System (GLOSA) uses V2I communication to guide drivers with speed advice for the vehicle to arrive at an upcoming intersection by the next green light (Stebbins, Hickman, Kim, & Vu, 2017; Stevanovic, Stevanovic, & Kergaye, 2013). Stop Sign Gap Assist (SSGA) utilizes V2I communication to warn drivers of a potential collision at a two-way stop controlled intersection (USDOT, 2017). ASAS utilizes V2I communication to provide vehicles with advisory speed messages to prevent hard braking at a yellow or red signal (Njobelo et al., 2018). Stop Sign Violation Warning (SSVW) helps drivers to avoid the risks of violating a stop sign by broadcasting the presence and position of the stop sign to the in-vehicle-device (USDOT, 2017). Some of CV safety applications developed to improve pedestrian safety include the Mobile Accessible Pedestrian Signal System, the Pedestrian in Signalized Crosswalk Warning, and the Intersection Movement Assist application. Pedestrian in Signalized Crosswalk technology warns drivers of any potential conflicts with a pedestrian (USDOT, 2017).

Connected Vehicle Safety Application Benefits

CV safety applications are effective in crash reduction. More than 250,000 crashes and 2,000 fatalities can be potentially prevented by using RLVW and Pedestrian in Signalized Crosswalk Warning applications (Cronin, 2018). In addition, more than 169,000 crashes and 5,000 fatalities can be prevented by the curve speed warning application (Cronin, 2018). Traffic management applications can potentially reduce crash-related incidents by 25% on freeways (Cronin, 2018). ASAS can potentially reduce the number of hard-braking incidents by nearly 50% with a 100% CV market penetration rate (Njobelo et al., 2018).

Crash Precursors

Several studies have been conducted to evaluate the potential crash precursors. Evaluation of the safety effects of reducing the posted speed limit in urban residential roads using the full Bayesian model was described by Islam & El-Basyouny (2015). Results showed that reducing speed limits is an effective way of improving traffic safety (Islam & El-Basyouny, 2015). Estimation of the effect of increased speed limits on crash occurrence on rural highways, using the Bayesian technique, was examined by Sayed & Sacchi (2016). The results showed that a change in speed limit led to a statistically significant increase in fatal-plus-injury crashes on highways of about 11.1% (Sayed & Sacchi, 2016). Flow characteristics that lead to traffic crashes on freeways was examined by C. Lee, Saccomanno, & Hellinga (2002). The results suggested that traffic density and variation of speed were statistically significant crash precursors, after controlling for the roadway geometry, time of the day, and weather (C. Lee et al., 2002).

Based on literature review speed variability is one of the significant crash precursors. Therefore, this study used speed variability as a performance measure to examine the impacts of CV smartphone technology on traffic safety on the signalized study corridor using the speed harmonization strategy.

Data Analysis

Data Reduction Process

In this study, intersection approach vehicle travel speeds were extracted from the recorded video data. A distance of 400 ft from the stop-line was set as the speed segment length, greater than the suggested 264 ft minimum length for a roadway with a posted speed limit greater than 40 mph (Currin, 2001). Time to traverse the speed segment length was recorded for each observed vehicle, and the speed of each of the observed vehicle was calculated using Equation 4-1.

$$v = {}^{d}/_{1.47t} \qquad \text{Equation 4-1}$$

Where, V is the speed in miles per hour, d is the speed segment length in feet, and t is the recorded time in seconds.

Speed Harmonization

Speed harmonization is a traffic management strategy that is implemented to reduce speed differences (shockwaves) between vehicles in response to a certain traffic condition, such as downstream congestion, incidents, and weather (Dowling et al., 2016). Speed differences can be evaluated in two categories: speed difference between vehicles on a specific lane (intra-lane shockwave) and speed difference between vehicles on adjacent lanes (inter-lane shockwave).

There are limited studies on speed harmonization and CV technology. In these few studies, speed harmonization is evaluated as speed differences (shockwave) between vehicles on the downstream and upstream segment, using Shockwave theory, as shown in Equation 4-2 (Dowling et al., 2016).

$$v_s = \frac{(k_d * \overline{u_s}(k_d) - k_u * \overline{u_s}(k_u))}{(k_d - k_u)} \qquad \text{Equation 4-2}$$

$$\text{where } \overline{u_s} = \frac{nL}{\sum_{i=1}^{n} t_i}$$

Where:

v_s is the speed differences (shockwave) between downstream and upstream segment

k_d is the traffic density on the downstream segment

k_u is the traffic density on the upstream segment

$\overline{u_s}$ is the space-mean speed

L is the length of the segment

t_i is the time it takes for a vehicle i to traverse the road segment

In this study, the effectiveness of the CV smartphone technology on harmonizing speed in the vicinity of an intersection was evaluated. The main focus was to reduce speed differences (variability) between vehicles within a specific lane, so as to reduce the chance of rear-end collisions. Since Equation 4-2 focuses on speed harmonization on a freeway, a new equation for the evaluation of speed harmonization in the vicinity of an intersection is proposed. Equations 4-3 and 4-4 are the proposed equations for calculating speed differences (variability) between vehicles within a specific lane for mixed traffic and traditional traffic conditions, respectively. The speed differences (variability) between vehicles within a specific lane were calculated for each vehicle group based on the proximity to each other. Speed variability was calculated using Equations 4-3 and 4-4 for mixed traffic and traditional traffic, respectively. Descriptive statistics of the speed variability results for both mixed traffic with CVs and in traffic with TVs only are summarized in Tables 4-1 and 4-2, respectively.

$$\Delta V_{i,\text{CV Penetration}} = \sum_{i=1}^{m} \frac{[\sum_{k=1}^{n} V_j - \sum_{j=1}^{n} \frac{V_j}{n}]/n}{m} \qquad \text{Equation 4-3}$$

$$\Delta V_{i,TV} = \sum_{i=1}^{m} \frac{[\sum_{k=1}^{n} V_j - \sum_{j=1}^{n} \frac{V_j}{n}]/n}{m} \qquad \text{Equation 4-4}$$

Where

ΔV_i Is an average speed variability between vehicles within a specific lane,

m is the total number of observed vehicle groups, with similar CV penetration rate in the case of mixed traffic,

n is the total number of vehicles in the specific vehicle group, and

V_j is the speed of the individual vehicle.

Table 4-1: Speed Variability between CVs Within a Specific Lane Based on CV Penetration Rate

CV Penetration [%]	N	Average [mph]	Min [mph]	Max [mph]	Stdev [mph]
10	113	2.08	0.35	4.44	1.44
20	98	2.06	0.09	5.12	1.46
30	123	2.04	0.04	7.64	1.66
40	87	1.81	0.07	6.52	1.23
50	105	1.62	0.01	8.52	2.13
60	96	1.51	0.59	2.52	0.68
70	110	1.50	0.88	2.04	0.60
80	89	1.36	0.13	3.62	1.16
90	-	-	-	-	-
100	53	1.22	0.21	2.23	0.88

Note: N is the number of data points, Min is the minimum observed speed variability in mph, Max is the observed maximum speed variability in mph, and StDev is the standard deviation of the speed variability in mph.

Table 4-2: Descriptive Statistic of Speed Variability Between TVs Within a Specific Lane

N	Average [mph]	Min [mph]	Max [mph]	Stdev [mph]
138	3.13	0.54	9.48	2.595

Note: N is the number of data points, Min is the minimum observed speed variability in mph, Max is the observed maximum speed variability in mph, and StDev is the standard deviation of the speed variability in mph.

Performance of CV Smartphone Technology on Improving Driving Safety

To analyze the impact of CV smartphone technology on improving driving safety through speed harmonization, speed variability was considered as a performance indicator. Results of speed variability between vehicles within a specific lane for different CV penetration rates are shown in Figure 4-1.

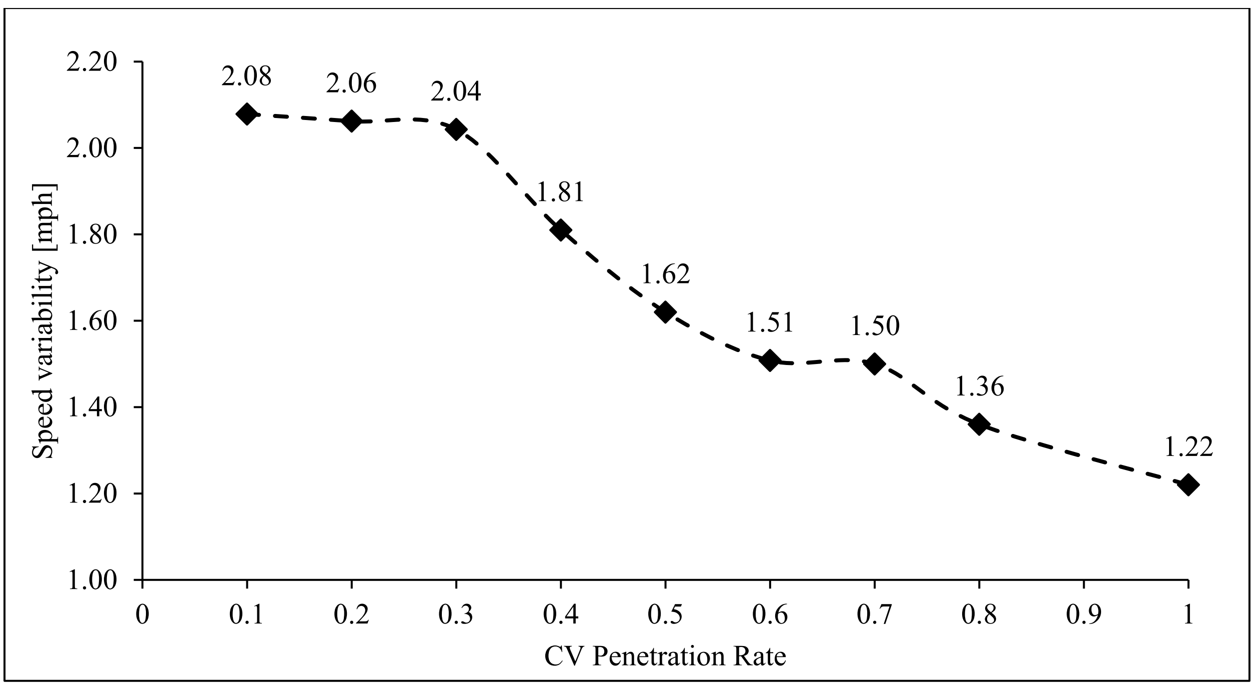

Figure 4-1: Speed variability between vehicles in a specific lane by CV penetration rate.

Statistical Analysis: Chi – Squared Test Method

Impacts of the CV smartphone application on traffic safety was evaluated based on its ability to harmonize speeds, especially when vehicles are approaching a signalized intersection. A safety evaluation was performed based on speed variability between vehicles within a specific lane. Statistical analysis was applied to determine if CV smartphone technology significantly reduced speed variability between vehicles within a specific lane. The Chi-Squared test method was used, due to its ability to make an inference about a population variance (McClave & Sincich, 2009), to determine if the speed variation of mixed traffic with CVs was statistically smaller than the speed variation of purely TVs. Before conducting the Chi-squared test, sample data for speed variation of both traffic conditions were tested for normalization, and the Anderson-Darling test results showed that the data were normally distributed.

The variance of the speed variability data of the mixed traffic, $\sigma^2_{\text{with CV}}$, was compared with the variance of the speed variability data of the TVs, σ^2_{TV} , under 95% confidence level to determine if $\sigma^2_{\text{with CV}} < \sigma^2_{\text{TV}}$ using the following null hypothesis:

H_o: $\sigma^2_{\text{with CV}} = \sigma^2_{\text{TV}}$ (The variance of the speed variability is the same for both traffic conditions)

H_a: $\sigma^2_{\text{with CV}} < \sigma^2_{\text{TV}}$ (The variance of the speed variability of the mixed traffic with CV is less than that of the traffic with entirely TVs)

The null hypothesis is rejected if $\chi^2_{\text{statistic}} < \chi^2_{0.05,\text{df}}$

The Chi-Squared test statistic was established using Equation 4-5.

$$\chi^2 = \frac{(n-1)\sigma^2_{\text{with CV}}}{\sigma^2_{\text{TV}}} \qquad \text{Equation 4-5}$$

The results of the Chi-Squared test, shown in Table 4-3, revealed that starting with 10% CV penetration, the speed variation of mixed traffic with CVs is significantly less than that of traffic consisting of entirely TVs.

Table 4-3: Summary of Chi-Squared Test Results

CV Penetration Rate [%]	N	Speed variability [mph]	Std. Dev [mph]	Variance	$\chi^2_{statistic}$	$\chi^2_{critical}$	Conclusion
10	113	2.08	1.44	2.074	34.488	88.570	SR
20	98	2.06	1.46	2.132	30.705	75.282	SR
30	123	2.04	1.66	2.756	49.923	97.493	SR
40	87	1.81	1.23	1.513	19.321	65.623	SR
50	105	1.62	2.13	4.537	70.068	81.468	SR
60	96	1.51	0.68	0.462	6.523	73.520	SR
70	110	1.5	0.6	0.360	5.827	85.903	SR
80	89	1.36	1.16	1.346	17.584	67.373	SR
100	53	1.22	0.88	0.774	5.980	36.437	SR

Note: N stands for the number of data points, Std. Dev is the standard deviation of the data, and SR stands for significant reduction.

Discussion of the Results

Speed variability between vehicles within a specific lane was found to decrease with an increase in CV penetration rate. Nassim et al. (2016) found similar results in a study on shockwave suppression by V2V communication, where the shockwave decreased with an increase in the CV penetration rate (Motamedidehkordi, Margreiter, & Benz, 2016). Speed variability between vehicles remained approximately constant with an increase in CV penetration to up to 30%. A decrease in speed variability between vehicles was observed when the CV penetration rate increased from 30% to 60%. A similar trend was observed on delay reduction presented by Ramezani et al. (2015), where, a sudden decrease in delay reduction was observed when the CV penetration rate increased from 70% to 80% . However, the study found no specific trend in the observed minimum, maximum, and standard deviation of the speed variability with the increase in CV penetration rate. Speed variability reduction of 61% was observed at 100% CV penetration rate, which is equivalent to a reduction of about 2.0 mph in speed variability between CV and TV traffic conditions. A similar observation was found by Waller, Ng, Ferguson, Nezamuddin, & Sun (2009), where with a variable speed limit of 45 mph, the effect of speed harmonization on speed variability reduction of about 2.25 mph was observed for the uncongested traffic model. The CV penetration rate of at least 10% is required to observe a significant speed variability reduction between vehicles in a specific lane. Similar findings were presented by Dowling et al. (2016), whereby with at least 10% CV penetration, a significant reduction in the magnitude of the speed drops was observed. This result is considered as safety benefit, by reducing the probability of traffic collisions.

Economic Costs Savings Analysis

The first step in performing the costs saving analysis was to determine the target crash types that could potentially be prevented by using the CV smartphone technology. Due to the type of CV technology used in this study (smartphone-based), three target crash groups were considered for analysis: lane-change crashes, rear-end collisions, and crossing-path collisions.

To understand how these targeted crash groups could be prevented, the CV smartphone application was mapped with pre-crash scenarios for each target crash group. These pre-crash scenarios were among the new typology of 37 pre-crash scenarios for crash avoidance research as described by Najm, Smith, & Yanagisawa (2007). As listed in Table 4-4, CV smartphone technology could potentially prevent at least one of four lane-change pre-crash scenarios considered, one of seven crossing-path pre-crash scenarios considered, and all five types of rear-end pre-crash scenarios considered in the study.

Table 4-4: Potentially Preventable Crash Types with CV Smartphone Technology

Crash Type	Pre-Crash Scenario
Rear-end Collision	Following Vehicle Making a Maneuver Following Vehicle Accelerating Following Vehicle Moving at Lower Constant Speed Following Vehicle Decelerating Following Vehicle Stopped
Lane Change Collision	Vehicle changing Lanes-Same Direction
Crossing-Path Collision	Running Red Light

The next step in the analysis was to determine the maximum number of crashes that could potentially be prevented by using CV smartphone technology. In this step, two things were determined: 1) the effectiveness of CV smartphone technology on crash reduction, and 2) the total number of crashes that occurred for each target crash group in the most recent year (2018).

The effectiveness of CV smartphone technology on crash reduction was evaluated based on the field tests, the most ideal method for obtaining actual effectiveness (T. Li & Kockelman, 2016). Based on the results from the field test, the effectiveness of CV smartphone technology on the selected pre-crash scenarios resulted in a nearly 60% reduction in fatal crashes at 100% CV penetration. The effectiveness of CV smartphone technology on reducing other crash severity types was developed based on the KABCO scale, where effectiveness increases 10% to the next lower level of severity, with the highest value being 100% for no injury crashes (FDOT, 2015). The KABCO scale records crash severity that resulted in death as K (for kill), an incapacitating (severe) injury as A, a non- incapacitating (moderate) injury as B, a possible (minor) injury as C, or no injury (property damage only) as O (FDOT, 2015). Therefore, as shown in Table 4-5, the effectiveness of the CV smartphone technology for non-fatal crash types will increase by 10% from to the next higher severity level (FDOT, 2015).

Table 4-5: Effectiveness of CV Smartphone Technology in Reducing Crashes

Safety Application	KABCO Severity Type					
	K	A	B	C	O	U
CV Smartphone Safety Application	0.6	0.7	0.8	0.9	1	1

Note: U stands for Unknown Injury.

Total number of crashes for each target crash group was obtained from 2018 crash reports obtained from the Signal Four Analytics database. To appreciate the safety benefits of the CV smartphone technology, the analysis was performed for the study corridor and statewide. Crash data for both the study corridor and the state are summarized in Table 4-6.

Table 4-6: 2018 Annual Crash Report Data from Signal Four Analytics Database

Crash Type	Crash Severity					
	No-Injury	Non-Traffic Fatality	Possible Injury	Non-Incapacitating Injury	Incapacitating Injury	Fatal Within 30 Days
Study Corridor						
Rear-End	100	0	37	11	1	0
Lane Change	39	0	3	1	0	0
Crossing Paths	7	0	2	1	0	0
Statewide						
Rear-End	44,956	8	11,956	4,040	844	49
Lane Change	13,363	1	1,202	1,189	182	14
Crossing Paths	18,920	10	8,259	3,704	1,004	121

The next step was to estimate the benefit associated costs with crash reduction. Since there is no cost associated with equipping the vehicle with the CV smartphone technology, the benefit associated with the crash reduction was estimated by multiplying the effectiveness of the CV smartphone application on corresponding crash severity and the total cost associated with each crash severity.

The crash costs associated with each crash severity, listed in Table 4-7, was obtained from Table 23.5.2 in the design exceptions and design variations manual, provided by FDOT from the Crash Analysis Reporting (C.A.R) System (FDOT, 2015).

Table 4-7: FDOT KABCO Crash Costs

Crash Severity	**Comprehensive Crash Costs**
Fatal (K)	$10,120,000
Severe Injury/ An Incapacitating Injury (A)	$574,080
Moderate Injury/ Non-Incapacitating Injury (B)	$155,480
Minor Injury/ A Possible Injury (C)	$96,600
Property Damage Only (O)	$7,600

Tables 4-8 and 4-9 summarize the estimated total costs of each crash severity and the economic cost benefit resulting from CV smartphone technology deployment. The results are categorized by study corridor and statewide.

Table 4-8: Estimated Annual Crash Costs by Severity Type Based on KABCO Crash Costs

Crash Type	**Crash Severity**					
	No-Injury	Non-Traffic Fatality	Possible Injury	Non-Incapacitating Injury	Incapacitating Injury	Fatal Within 30 Days
Study Corridor						
Rear-End	$0.760M	$0	$3.574M	$1.710M	$0.574M	$0
Sideswipe	$0.296M	$0	$0.290M	$0.155M	$0	$0
Crossing Paths	$0.053M	$0	$0.193M	$0.155M	$0	$0
Statewide						
Rear-End	$342M	$81M	$1,155M	$628M	$485M	$496M
Sideswipe	$102M	$10M	$116M	$185M	$104M	$142M
Crossing Paths	$144M	$101M	$798M	$576M	$576M	$1,225M

Table 4-9: Estimated Annual Economic Costs Savings of Deploying CV Smartphone Technology with 100 Percent CV Market Penetration

Crash Type	Crash Severity					
	No-Injury	Non-Traffic Fatality	Possible Injury	Non-Incapacitating Injury	Incapacitating Injury	Fatal Within 30 Days
Study Corridor						
Rear-End	$0.760M	$0	$3.21M	$1.368M	$0.40M	$0
Sideswipe	$0.296M	$0	$0.26M	$0.124M	$0	$0
Crossing Paths	$0.053M	$0	$0.174M	$0.124M	$0	$0
Statewide						
Rear-End	$342M	$49M	$1,039M	$503M	$339M	$298M
Sideswipe	$102M	$6M	$105M	$148M	$73M	$85M
Crossing Paths	$144M	$60M	$718M	$461M	$403M	$735M

Results of the Economic Costs Savings Analysis

CV smartphone technology could prevent 60% of all fatalities in their respective target crash groups, resulting in a potential annual cost savings of about $1.2 billion statewide. About 70% of all severe injury crashes could be reduced, which is equivalent to an economic cost savings of about $0.4 million and $816 million at the study site and statewide, respectively. Economic cost savings of about $6.4 million and $3.6 billion could be realized from other crash severity types, including property damaged only, if the CV smartphone technology is deployed. Of the three target crash groups evaluated, the CV smartphone technology provided more annual cost savings in reducing rear-end crash occurrence of about $5.75 million and $2.6 billion annually at the study site and statewide, respectively. This is due to the relatively large number of crashes that the CV smartphone technology addressed.

CHAPTER 5 TRAFFIC OPERATION EVALUATION: SIMULATION APPROACH

Introduction

Field tests explained in Chapter three of this thesis addressed the impact of CV smartphone technology only on start-up lost times. Other MOEs that address the impact of CV technology on traffic operation could not easily be evaluated using methods adopted to evaluate the field test data. These MOEs include: vehicle control delay, vehicle stop delays, and fuel consumption. Therefore, a simulation approach, based on field observations, was adopted to evaluate the impact of CV smartphone technology on these MOEs.

Methodology

Procedural steps adopted to evaluate the impact of CV smartphone technology on traffic operation using the microscopic simulation tool “Vissim” include: base model development, base model verification and validation, base model calibration, and data analysis of the selected MOEs. These procedures are explained as follows:

Base Model Development

Development of a traffic microsimulation model that replicates the existing traffic characteristics of a specified study area is key to the success of any traffic microsimulation study. The base model serves as a footprint from which other alternatives are based on. This study used the procedure recommended by the FDOT Traffic Analysis Handbook (FDOT, 2014) to develop the base model of the study site. The procedure is summarized in Appendix A.

Base Model Verification

Efficient model calibration can be attributed to the development of an error-free base model. Therefore, model verification was performed to ensure the base model did not contain errors. The verification process used followed the Vissim Model Error Checking checklist provided in Table 7-6 of the FDOT Traffic Analysis Handbook (FDOT, 2014), and described in Appendix B.

Model Calibration

For microsimulation analysis, FDOT suggests that MOEs to be used for calibration should include capacity, traffic volumes, and at least two other MOEs (FDOT, 2014). In this study, traffic volume, travel speeds, travel time, and saturation headways were used for model calibration. The procedure used to calibrate each of the selected MOEs is described in Appendix C**.**

Data Analysis

Various measure of effectiveness (MOE) were used to evaluate the impact of CV smartphone technology on a signalized corridor. These MOEs include; vehicle travel times, vehicle control delay, vehicle stop delay, number of vehicles stop, queue length, and fuel consumption.

Vehicle Travel times

Vehicle travel time was measured in Vissim by coding the vehicle travel time measurement object at the beginning and end of the target segment. The results are presented for each analysis segment and for the overall analysis corridor in Table 5-1.

Table 5-1: Simulation Results of Vehicle Travel Times at Different CV Penetration Rate.

CV Penetration Rate	Travel times [sec]					Percentage Increase in Travel Times
	1	2	3	4	NB direction from 1-4	
0	9.77	39.42	33.58	25.88	117.6	0.00%
10	9.77	40.63	33.15	25.17	118.23	0.54%
20	9.75	42.07	32.87	25.15	118.65	0.89%
30	9.75	43.64	32.73	25.09	123.73	5.21%
40	9.79	44.94	33.77	25.12	123.73	5.21%
50	9.82	46.03	35.70	25.20	129.23	9.89%
60	9.87	47.22	38.32	25.25	138.80	18.03%
70	9.93	47.95	40.72	25.26	145.65	23.85%
80	9.97	49.33	44.59	25.30	158.64	34.90%
90	10.01	50.45	48.36	25.39	166.80	41.84%
100	10.09	51.34	53.95	25.59	177.90	51.28%
Percentage Travel Times Increase	3.28%	30.24%	60.66%	-1.12%		
Overall Intersection Delay [s/veh]	9.09	19.17	28.97	9.06		
Overall Intersection LOS	A	B	C	A		

Node Evaluation

All selected MOEs, except vehicle travel times, were evaluated in Vissim using node evaluation. The node evaluation was configured by defining the start of delay segment and queue conditions. For each intersection approach, the start of delay segment depends on the length between the two intersections. Queue conditions were defined by providing the speed that defines the beginning and end of the queue. Also, maximum headway and the maximum length to be evaluated was defined. Fuel consumption was measured based on the Traffic Network Study Tool, Version 7F (TRANSYT-7F) methodology, for emission and fuel consumption. The TRANSYT- 7F estimates fuel consumption based on a linear combination of vehicle travel time, vehicle delay, and vehicle stops (IHS Global Inc., 2017). The regression model used is described in Equation 5-1.

$$\mathrm{F} = \mathrm{K_{i1}} * \mathrm{TT} + \mathrm{K_{i2}} * \mathrm{D} + \mathrm{K_{i3}} * \mathrm{S} \qquad \text{Equation 5-1}$$

Where,

F = fuel consumed in US gallons per hour

TT = total travel in vehicle miles per hour

D = total delay in vehicle-hour per hour

S = total vehicles stop per hour

K_{ij} = model coefficients based on cruise speed on each link.

Tables 5-2 through 5-5 summarize the simulation results of the node evaluated MOEs, i.e., queue length, number of vehicles stop, fuel consumption, vehicle control delay, and vehicle stop delay. These results are also presented graphically in Figures 5-1 through 5-4.

Table 5-2: Simulation Results of MOEs at NB Approach of SR 121 and Windmeadows Blvd.

CV penetration	Queue Length [ft]	Number of vehicle stops per 100 vehicles	Fuel Consumption [gallons]	Vehicle Delay [s/veh]	Stop Delay [s/veh]
0	153.49	33	10.18	5.71	1.36
10	151.00	28	9.43	5.71	1.14
20	140.00	23	8.62	5.44	0.91
30	126.72	20	7.98	5.19	0.74
40	116.91	17	7.54	5.00	0.60
50	105.00	15	7.15	4.82	0.49
60	100.00	14	6.88	4.66	0.38
70	95.00	13	6.76	4.55	0.30
80	86.00	11	6.50	4.42	0.21
90	75.00	10	6.31	4.29	0.13
100	73.70	10	6.19	4.23	0.07

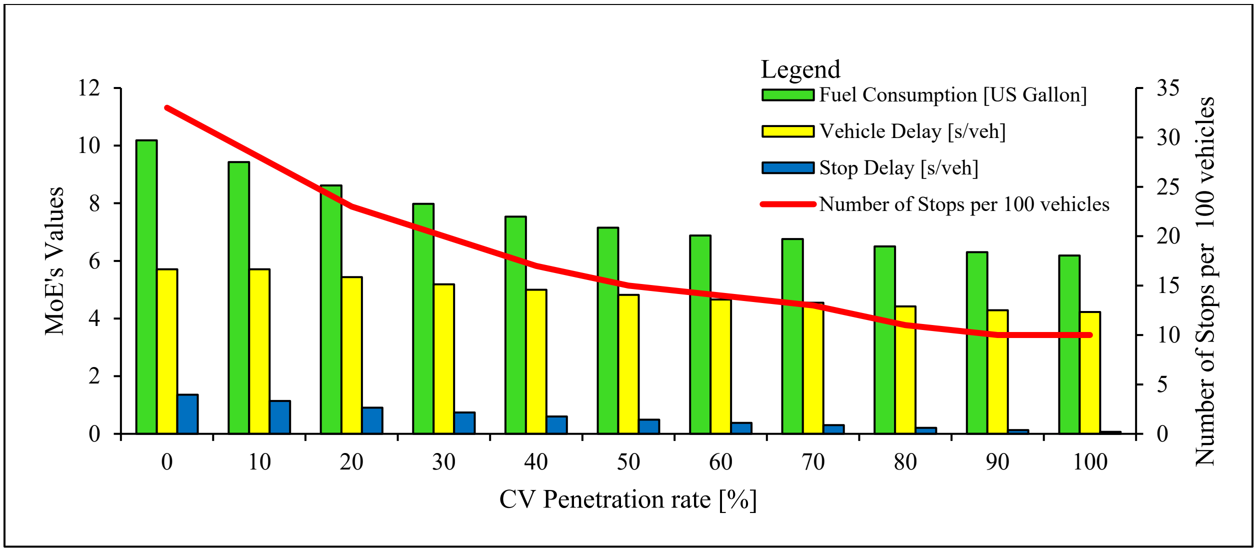

Figure 5-1: Simulation results of MOEs at NB approach of SR 121 and Windmeadows.

Table 5-3: Simulation Results Summary of MOEs at NB Approach of SR 121 and 20th Ave.

CV penetration	Queue Length [ft]	Number of Vehicle Stops per 100 vehicles	Fuel Consumption [gallons]	Vehicle Delay [s/veh]	Stop Delay [s/veh]
0	162.63	47	5.83	22.90	17.78
10	133.00	35	5.38	20.16	15.37
20	129.27	26	5.02	17.24	13.13
30	114.80	21	4.92	15.48	11.74
40	92.41	18	4.86	13.94	10.57
50	83.77	17	4.83	12.75	9.64
60	76.23	15	4.79	11.72	8.84
70	73.00	14	4.69	10.84	8.07
80	70.00	13	4.83	10.45	7.71
90	67.57	12	4.85	9.75	7.08
100	65.80	12	4.91	9.36	6.56

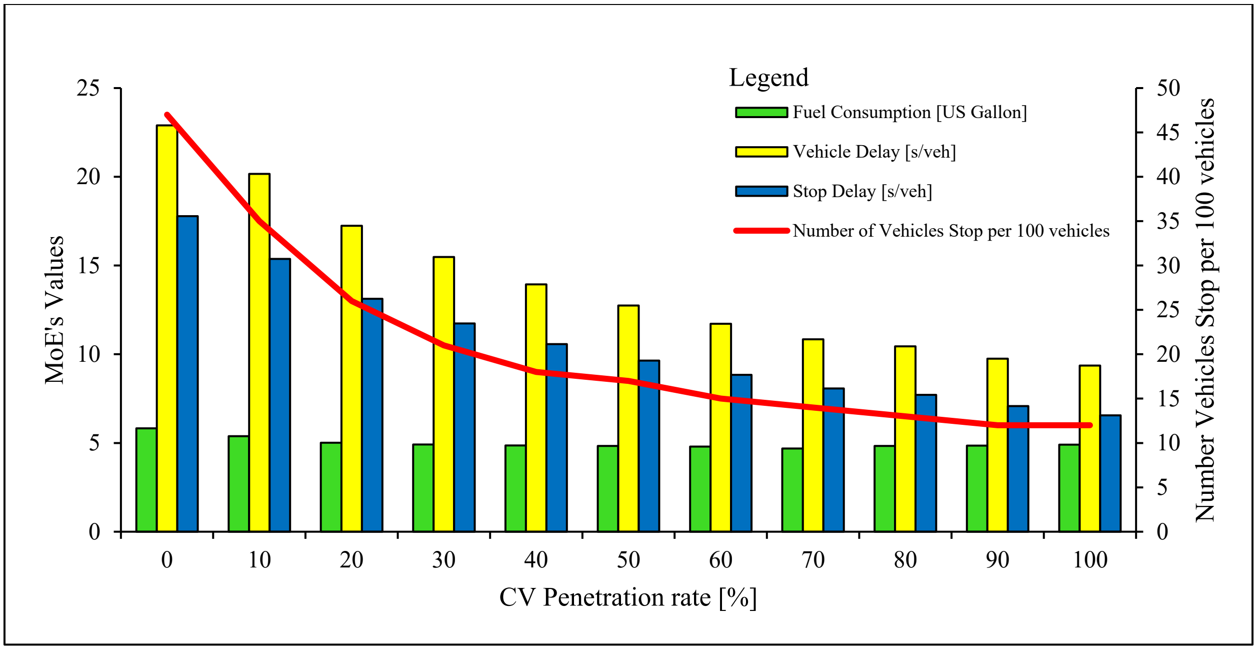

Figure 5-2: Simulation results of MOEs at NB approach of SR 121 and 20TH Ave.

Table 5-4: Simulation Results Summary of MOEs at NB Approach of SR 121 and Hull Rd

CV penetration	Queue Length [ft]	Number of Vehicle Stops per 100 vehicles	Fuel Consumption [gallons]	Vehicle Delay [s/veh]	Stop Delay [s/veh]
0	218.87	70	12.93	27.53	18.82
10	210.23	61	12.19	24.67	16.58
20	201.22	51	11.29	21.87	14.41
30	198.79	41	10.31	18.94	12.08
40	196.32	37	10.06	17.94	11.33
50	221.35	37	10.40	18.17	11.59
60	240.07	37	10.88	19.08	12.23
70	253.29	39	11.56	20.28	13.06
80	283.39	42	12.58	21.96	14.23
90	288.64	44	13.62	23.61	15.27
100	321.50	53	15.45	25.94	16.56

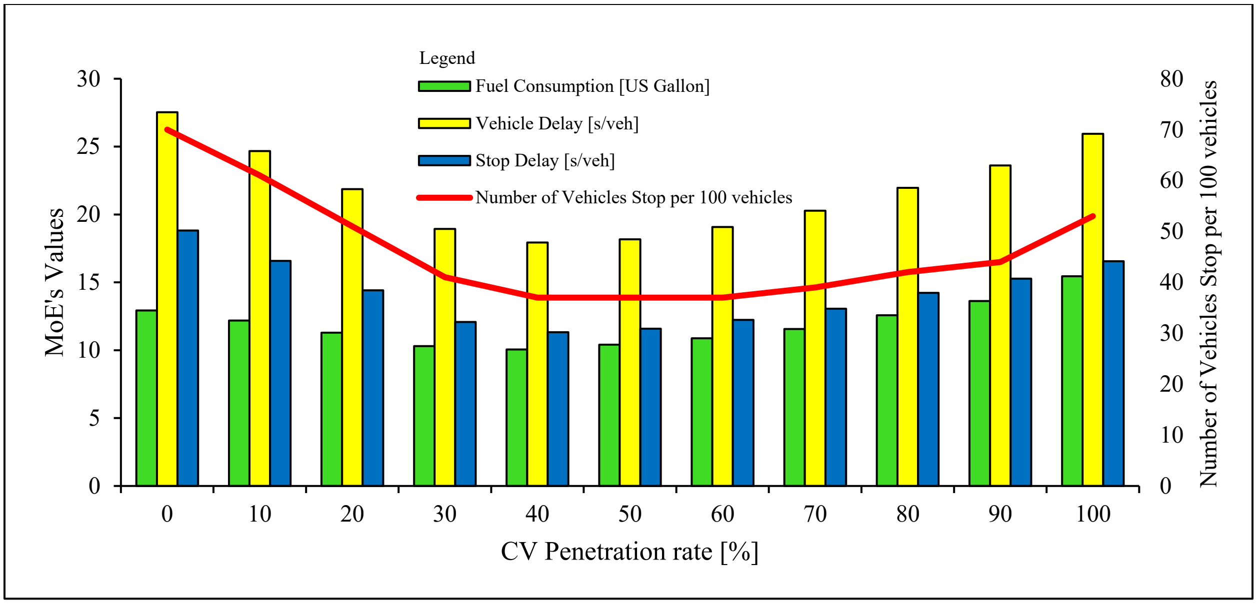

Figure 5-3: Simulation results of MOEs at NB approach of SR 121 and Hull Rd.

Table 5-5: Simulation Results Summary of MOEs at NB Approach of SR121 and Radio Rd

CV penetration	Queue Length [ft]	Number of Vehicle Stops per 100 vehicles	Fuel Consumption [gallons]	Vehicle Delay [s/veh]	Stop Delay [s/veh]
0	55.24	6	2.857	3.64	2.56
10	52.12	6	2.592	3.47	2.55
20	55.32	6	2.72	3.35	2.44
30	54.38	5	2.835	3.16	2.27
40	54.81	5	2.856	2.94	2.08
50	50.10	5	2.903	2.79	1.97
60	49.95	5	2.972	2.71	1.88
70	50.11	4	2.987	2.58	1.76
80	49.75	4	3.012	2.49	1.68
90	46.16	4	3.049	2.32	1.52
100	46.23	4	3.067	2.26	1.5

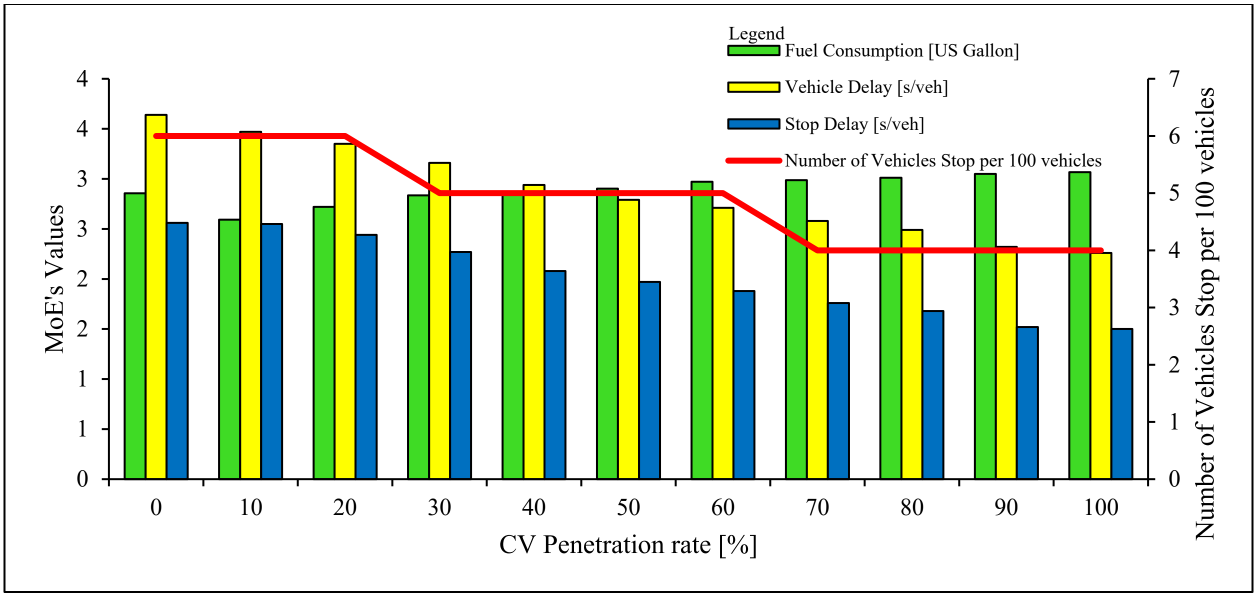

Figure 5-4: Simulation results of MOEs at NB approach of SR 121 and Radio Rd.

Discussion of the Results

Vehicle Travel Times

Simulation results of the vehicle travel times for each segment between intersections, as well as the entire analysis-corridor, between Windmeadows Blvd and Radio Rd, were evaluated and summarized in Table 5-1. At 100 percent CV penetration rate, a 3.28%, 30.24%, 60.66%, and -1.12% increase in travel time was observed for each respective segment, compared to the TV travel time, as noted in Table 5-1. Furthermore, vehicle travel times for the entire analysis-corridor was observed to increase as the CV penetration rate increased, with an increase of about 51% at 100 percent CV penetration (see Table 5-1).

Vehicle Delays at Intersections

Vehicle control delay and vehicle stop delay were also evaluated as a MOE of CV smartphone technology on a signalized corridor. Results are presented in Tables 5-2 through 5-5. At 100 percent CV penetration, a reduction of 26% in vehicle control delay and 95% in vehicle stop delay was observed in the NB approach of the SR 121 and Windmeadows Blvd intersection (see Table

5-2). Similarly, at 100 percent CV penetration rate, a reduction of 59% in vehicle control delay and 63% vehicle stop delay was observed at the NB approach of the SR 121 and 20th Ave intersection (see Table 5-3). A reduction of 6% in vehicle control delay and 12% in vehicle stop delay was observed at 100 percent CV penetration at the NB approach of the SR 121 and Hull Rd intersection (see Table 5-4). However, a maximum reduction of about 40% and 35% in vehicle control delay and vehicle stop delay, respectively, was observed at this intersection at a 40 percent CV penetration rate. Lastly, a reduction of 38% in vehicle control delay and 41% in vehicle stop delay, at 100 percent CV penetration, was observed at the NB approach of the SR 121 and Radio Rd intersection (see Table 5-5).

Vehicle Queue Length

Vehicle queue length formed at an intersection was used as one of the MOEs of CV smartphone technology on a signalized corridor. Simulation results of the vehicle queue length formed at each intersection analysis-approach is summarized in Tables 5-2 through 5-5. At 100 percent CV penetration, a reduction of about 52% in vehicle queue length was observed at the NB approach of the SR 121 and Windmeadows Blvd intersection (see Table 5-2). Similarly, at 100 percent CV penetration, a reduction of 60% in vehicle queue length was observed at the NB approach of the SR 121 and 20th Ave intersection (see Table 5-3). An increase of about 47% in vehicle queue length at 100 percent CV penetration was observed at the NB approach of the SR 121 and Hull Rd intersection (see Table 5-4). However, a maximum reduction of about 10% in vehicle queue length was observed at this intersection at the 40 percent CV penetration rate. Lastly, a reduction of 16% in vehicle queue length was observed at 100 percent CV penetration at the NB approach of the SR 121 and Radio Rd intersection (see Table 5-5).

Number of Vehicle Stops

The primary goal of utilizing the vehicle speed advisory provided by CV smartphone technology is to reduce the stop-and-go movement at a signalized intersection. Therefore, it was important to evaluate the effectiveness of CV smartphone technology in reducing the number of vehicle stops due to red signal at an intersection. In Vissim, the number of vehicle stops due to red light is evaluated as the number of vehicle stops per vehicle. Simulation results are summarized in Tables 5-2 through 5-5, and show the number of vehicle stops, due to a red light, per 100 vehicles in each analysis-approach. At the 100 percent CV penetration rate, a reduction of 70% in the number of vehicle stops was observed at the NB approach of the SR 121 and Windmeadows Blvd intersection (see Table 5-2). Similarly, a reduction of 74% in the number of vehicle stops was observed at the NB approach of the SR 121 and 20th Ave intersection, at 100 percent CV penetration (see Table 5-3). A reduction of about 24% in the number of vehicle stops per 100 vehicles, at 100 percent CV penetration, was observed at the NB approach of the SR 121 and Hull Rd intersection (see Table 5-4). However, a maximum reduction of about 47% in the number of vehicle stops per 100 vehicles was observed at this intersection at 40 percent CV penetration rate. Lastly, a reduction of 33% in the number of vehicle stops per 100 vehicles was observed at the NB approach of the SR 121 and Radio Rd intersection (see Table 5-5).

Fuel Consumption

Vehicle fuel consumption in the analysis-segment of each intersection was used as one of the MOEs of the CV smartphone technology on a signalized corridor. Vissim reports vehicle fuel consumptions in terms of gallons. Simulation results of vehicle fuel consumptions in the analysis-approach at each intersection is summarized in Tables 5-2 through 5-5. At a 100 percent CV penetration rate, a reduction of 39% in vehicle fuel consumption was observed at the NB approach of the SR 121 and Windmeadows Blvd intersection (see Table 5-2). Similarly, at 100 percent CV penetration, a reduction of 16% in vehicle fuel consumption was observed at the NB approach of the SR 121 and 20th Ave intersection (see Table 5-3). The increase of about 19% in vehicle fuel consumption at 100 percent CV penetration was observed at the NB approach of the SR 121 and Hull Rd intersection (see Table 5-4). However, a maximum reduction of about 22% in vehicle fuel consumption was observed at this intersection at 30 percent CV penetration. Lastly, an increase of 7% and a maximum reduction of about 9% in vehicle fuel consumption, at 100 percent and 10 percent CV penetration, respectively, was observed at the NB approach of the SR 121 and Radio Rd intersection (see Table 5-5).

CHAPTER 6 FINDINGS

Impact of CV Smartphone Technology on Start-up Lost Time and Discharge Headway Distribution Model

Discharge headways of the first ten vehicles in a standing queue were evaluated from the field data observed for the two traffic conditions under consideration (i.e., entirely TVs, and mixed traffic of TVs and CVs). Based on statistical analyses, the second discharge headway seemed to follow a different distribution compared to the other discharge headways, for both traffic conditions. The second distribution of discharge headway is the negatively skewed while other discharge headways have a positive skewed distribution (see Tables 3-1 and 3-2). This implies that most of the second queued vehicles have a larger discharge headway than any of the first four vehicles. Literature reviewed termed this finding as "second vehicle delay phenomenon", which contradicts the fact that the second queued vehicle will generally have a smaller headway than the first queued vehicle, and the rest of the vehicles will have a slightly lower headway than the preceding vehicle. Many studies have suggested deploying signal countdown timers to resolve this problem. However, results in this study showed that the for both traffic conditions (i.e., entirely TVs, and mixed traffic of TVs and CVs), the same distribution for the second discharged headways was observed. Regardless of the presence of traffic signal countdown timers, the second queued vehicle cannot respond to signal changes at the same time as the first queued vehicle. Therefore, the presence of traffic signal countdown timers alone is not a viable solution to the problem.

Impact of CV Smartphone Technology on Driving Safety

The impact of CV smartphone technology on driving safety was evaluated for the signalized study corridor, based on field observation data, using speed variability as the performance measure. Speed variability between vehicles within a specific lane was computed for each traffic condition (i.e., entirely TVs, and mixed traffic of TVs and CVs). In case of mixed traffic, speed variability was computed and grouped by CV penetration rate. Comparisons of speed variability between the two traffic conditions was completed, and the Chi-Squared test method was applied to determine the statistical differences between the two traffic conditions. The results showed the speed variation between vehicles within a specific lane in mixed traffic was significantly lower than that of TVs alone, suggesting that CV smartphone technology may improve driving safety. Results also indicate that an increase in the CV penetration rate may further increase driving safety. Driving safety improved rapidly from 30% to 60% CV penetration rates, with a fair improvement from 60% to 100% CV penetration. Findings showed that at least 10% CV penetration rate was enough to observe a significant improvement in driving safety.

Economic Cost Savings of CV Smartphone Technology

Based on field data evaluations, results indicate that CV smartphone technology may help to prevent 60% of fatalities in the target crash groups analyzed, resulting in an annual cost savings of about $1.2 billion statewide. The number of severe injury crashes could potentially be reduced by 70%, which is equivalent to an economic cost savings of approximately $0.4 million and $816 million at the study site and statewide, respectively. Cost savings of about $6.4 million and $3.6 billion may be realized from other crash severity types, including property damaged only crashes, if CV smartphone technology is deployed. Of the three target crash groups evaluated, CV smartphone technology provided more annual cost savings in reducing rear-end crash costs by nearly $5.75 million and $2.6 billion annually at the study site and statewide, respectively. These savings reflect the large number of crashes that the CV smartphone technology can address.

Findings from the Microscopic Simulation Analysis

Driving behaviors, observed in the field for the two traffic conditions (i.e. entirely TV and mixed traffic of TV and CV), were modeled using Vissim software. The MOEs selected for calibration included traffic volumes, travel speed, travel times, and discharge headways. The ultimate goal was to determine the car-following model of the CVs in mixed traffic. Three parameters of the arterial car-following model (Wiedemann 74) changed, including the average standstill distance, the additive part of the safety distance, and the multiplicative part of safety distance. The resulting values of the average standstill distance were 6.56 ft and 4.0 ft for TVs and CVs in mixed traffic conditions, respectively. The resulting additive part of safety distance was 3.0 and 2.5 for TVs and CVs in mixed traffic conditions, respectively. Resulting values of 4.25 and 4.30 for TVs and CVs in mixed traffic conditions, respectively, were found for the multiplicative part of safety distance.

Based on microsimulation results on travel times, CV smartphone technology provided more improvement to travel times along corridors consisting of intersections for facilities with a LOS of B. The results revealed an increase in travel times when the LOS of the intersection decreased. This finding is due to the advisory speeds, delivered to the driver by the CV smartphone technology, not considering the effect of the queue formed at an intersection. As the intersection LOS decreases, longer queues are formed, which impacts the efficiency of CV smartphone technology. Analyses corroborated this factor showing an increase in vehicle travel times on segments approaching the intersection that operated at a lower LOS, i.e., an average of about 1%, 3%, 30%, and 61% increase in travel time was found along segments approaching intersections operating at a LOS of A, A, B, and C, respectively.

CV smartphone technology was found to improve intersection performance in terms of vehicle delays, regardless of the LOS. However, the quantitative efficiency of CV smartphone technology on improving intersection performance in terms of vehicle delay depends on the intersection LOS. It was observed that with an intersection LOS of at least a B or higher, efficiency of CV smartphone technology on improving intersection performance in terms of vehicle delay increased with the increase in CV penetration, with the maximum efficiency observed at 100 percent CV penetration rate. However, for intersections with a LOS of C or lower, the efficiency of CV smartphone technology on improving intersection performance, in terms of vehicle delay, increases up to a certain CV penetration rate, and then starts to decrease again.

The maximum improvement of 40% in vehicle control delay and 35% in vehicle stop delay was observed at 40 percent CV penetration at the NB approach of the SR 121 and Hull Rd intersection. CV penetration rates ranging from 30 to 60 percent was observed to improve the approach LOS from a LOS C to a LOS B.

Similar findings were observed from the microscopic simulation of vehicle queue length formed at an intersection, number of vehicle stops per 100 vehicles in the analysis segment, and the vehicle fuel consumption in the analysis segment. However, an interesting finding was observed in terms of vehicle fuel consumption in the analysis segment when the number of vehicle stops due to a red light per 100 vehicles was less than six for the TVs only traffic condition. Although the intersection was operating at a LOS A, the effectiveness of CV smartphone technology on reducing fuel consumption was observed to increase up to a certain value and then decrease as the CV penetration rate increased. This finding suggests that if an intersection approach segment has six or fewer vehicle stops per 100 vehicles, implementing CV smartphone technology on that segment will not contribute to increased savings in terms of vehicle fuel consumption.

CHAPTER 7 CONCLUSIONS AND RECOMMENDATIONS

This thesis evaluated the effectiveness of CV technology on improving traffic mobility and safety at signalized intersections. The CV smartphone technology, developed by Connected Signals, Inc. and utilizes a smartphone application, called Enlighten, in place of a vehicle OBU, was selected to conduct the research. The study was based on field observations obtained from a 1.1 mile segment of SR 121 (SW 34th Street) in Gainesville, Florida, which includes five intersections.

The effectiveness of CV smartphone technology on traffic mobility was evaluated by examining its impact on start-up lost time and distribution models of discharge headways. The evaluation considered two different traffic conditions: 1) traffic consisting of entirely TVs, and 2) mixed traffic consisting of both CVs and TVs.

Field recorded discharge headways revealed that CV smartphone technology has a positive impact on the traffic mobility. The average start-up lost time for CV enabled vehicles was found to be 0.27 seconds, an 86% reduction, while the average start-up lost time for TVs was observed to be 1.93 seconds.

The impact of CV smartphone technology on the distribution model of the discharge headways was attributed to findings by Sharma et al. (2009), which suggested that the presence of a traffic signal countdown timer affects the distribution of discharge headways. This thesis found that CV smartphone technology had no impact of on a specific distribution model of the discharge headways for the first four queued vehicles. However, a shift in the peak discharge of the TV and CV distributions, of the same queued position, was observed. This observation would account for the reduction in start-up lost time. Peak shifts of about 62%, 36%, 15%, and 13% for the first four queue positions, respectively, were observed, and each represents a reduction in start-up lost time.

Impacts of CV smartphone technology on driving safety was evaluated by examining the technology's ability to harmonize speed. Speed variability was used as the MOE in this study. Results found that deployment of CV smartphone technology may improve driving safety by reducing speed variability between vehicles within a specific lane by 48%, 56%, and 61% at CV market penetration rates of 50%, 75% and 100%, respectively.

Deploying CV smartphone technology could result in an average total economic cost savings associated with crashes of approximately $6.8 million for the study corridor and $5.6 billion statewide. These results are based on the economic cost savings analyses of target crash groups (i.e., lane-change crashes, rear-end collisions, and crossing-path collisions) that occurred in the year 2018. Additionally, CV smartphone technology provided more annual benefit in reducing the number of rear-end crashes by approximately $5.74 million and $2.6 billion annually for the study corridor and statewide, respectively. These savings reflect the large number of crashes that the CV smartphone technology can address.

Using Vissim microsimulation software, this thesis developed and proposed an arterial car-following model of the traffic condition consisting of CVs in mixed traffic. The process of developing the car-following model involved developing and calibrating a Vissim model using driving behaviors observed in the field. These driving behaviors include: driver's reaction to signal changes, lane change behavior, and discharge headways of the first through the tenth queued vehicles. The developed CV arterial car-following model had a smaller average standstill distance of 4.0 ft, compared to both the default Vissim value of 6.56 ft and the resulting TV average standstill distance of 6.56 ft. The resulting additive part of safety distance in CV arterial car-following model was 2.5, which was smaller than 3.0 TV additive part of safety. The multiplicative part of safety (4.3) in the CV arterial car-following model was found to be slightly higher than in a TV arterial car-following model (4.25). All the resulted arterial car-following parameters for both TV and CV are within the suggested range by FDOT (FDOT, 2014).

Based on the microsimulation evaluation of the impact of CV smartphone technology on a signalized corridor, results suggests that CV smartphone technology provides greater benefits at intersections with a LOS of B or higher, compared to lower levels of service. For an intersection operating at a LOS of C, CV smartphone technology works better for CV penetration rates of 30 to 60 percent.

Findings from this thesis work will not only add to the body of knowledge related to CV technology, but also will be useful to transportation agencies as CV technology becomes increasingly more utilized in transportation management strategies. Traffic engineers and other traffic related agencies may also apply the research findings in planning and traffic operations efforts that involve CV technology.

There are several limitations on this thesis work. First, the field test was conducted during off-peak weekday traffic periods, during AM and PM hours. The second limitation relates to the economic cost savings analyses. Results obtained from the cost analyses were based on the assumption that the effectiveness of CV smartphone technology in potentially preventing fatal crashes translates to effectively improving driving safety. The third limitation is that research findings contained in this thesis may only be useful in states where cell phone usage while driving is not fully prohibited, and dashboard phone docking is allowed, at a minimum. Lastly, the fuel consumption results were derived from the Vissim node evaluation, which uses the Traffic Network Study Tool, version 7F (TRANSYT-7F) methodology to determine emission and fuel consumption. Since TRANSYT- 7F estimates fuel consumption based on a linear combination of vehicle travel time, vehicle delay, and vehicle stops, limitations may exist. Therefore, further research is suggested to evaluate the impact of CV smartphone technology on traffic mobility and safety during peak traffic periods. Further analysis of the financial benefits to transportation agencies when deploying this type of CV technology should also be considered.

APPENDIX A

Base Model Development

Creating a Scaled Base Model

The FDOT Traffic Analysis Handbook recommends that any base model be built from a scaled background image, such as, but not limited to, an orthorectified aerial image or Computer Aided Design and Drafting (CADD) image (FDOT, 2014). In Vissim, a scaled base model can be built using various methods. Scaled background images from Google maps may be imported, or available maps embedded within the Vissim software, such as Open street maps and Bing maps, may be used. For this study, the scaled base model was created from a Bing map following Vissim software guidelines (PTV, 2018). Figure A-1 provides several examples of aerial images retrieved from Bing maps, and used in the analyses.

Source: Bing map, 2019 (not to scale)

Figure A-1: Examples of Bing map scaled aerial images of study area intersections.

Coding Road Network Geometry

In Vissim, road network geometry is coded using the links and connectors available in the network editor. The scaled background image of the study site from the Bing map was used to provide accurate lane geometry and dimensions. Guidelines provided by PTV (2018) were followed to develop the coding links and connectors. During the process of coding roadway network geometry, the following parameters were considered:

- Corridor sections with similar geometry were coded with a single link, so as to minimize unnecessary segmentation along the corridor.
- Where segmentation was required, the overlap between link and connector were minimized, since overlaps tend to affect traffic flow in the network.
- Intersection turn bays were coded in such a way that all the turning movements occur across connectors.
- External links were coded (not too long) in such a way that demand volume was loaded into the model within the analysis time period.

Coding Desired Speed

In Vissim, the desired speed is coded using the speed distribution. Therefore, the empirical distribution of the desired speed was developed following guidelines suggested by Currin (2001). A roadway segment was selected for measuring the speed data based on the following criteria: (a) straight segments, and (b) sections long enough to avoid the influence of traffic signals on travel speeds. In this study, a 0.41 mile corridor along SW 34th Street (SR 121) between Windmeadows Blvd and 20th Ave was selected. The influence of heavy traffic on speed was avoided by collecting speed data for light traffic conditions. A 371 ft speed segment was used, which is greater than the minimum suggested length of 264 ft for a roadway with a posted speed limit greater than 40 mph suggested by Currin (2001) (see Table 2-1). Time to traverse the speed segment length was recorded for each observed vehicle, and the speed of each observed vehicle was calculated using Equation A-1. The resulting 50th and 85th percentile speeds were 48 mph and 53.62 mph, respectively.

$$v = {}^{d}/_{1.47t} \quad \text{Equation A-1}$$

Where, v is the speed in miles per hour, d is the speed trap length in feet, and t is the recorded time in seconds.

The goodness of fit test was conducted using the Anderson-Darling test. Based on the p-value and Anderson-Darling value, results suggests that the measured speed data follow a normal distribution in the field. The Anderson-Darling test results, descriptive statistics of the measured speed data are shown in Table A-1. The empirical cumulative frequency curve is shown in Figure A-2.

Table A-1: Descriptive Statistics and Goodness of Fit Results of Measured Speed Data

N	Mean	StDev	Median	Minimum	Maximum	Skewness	Kurtosis	AD	P-Value
153	48.03	5.27	48.00	33.32	59.40	-0.171	-0.152	0.233	0.794

Where N is number of observed vehicles, StDev is standard deviation of the measured speed data in mph, and AD is the Anderson-Darling value.

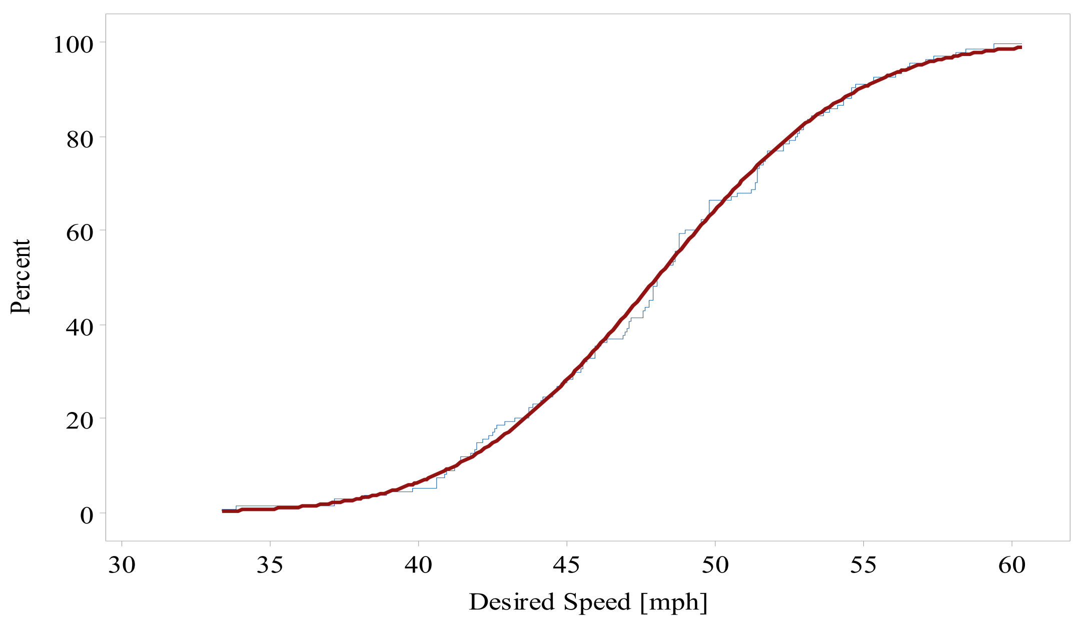

Figure A-2: Empirical CDF of the field observed desired speeds.

The developed empirical distribution was coded in Vissim following guidelines from PTV (2018). The Vissim coded desired speed distribution from the developed empirical cumulative frequency distribution is shown in Figure A-3.

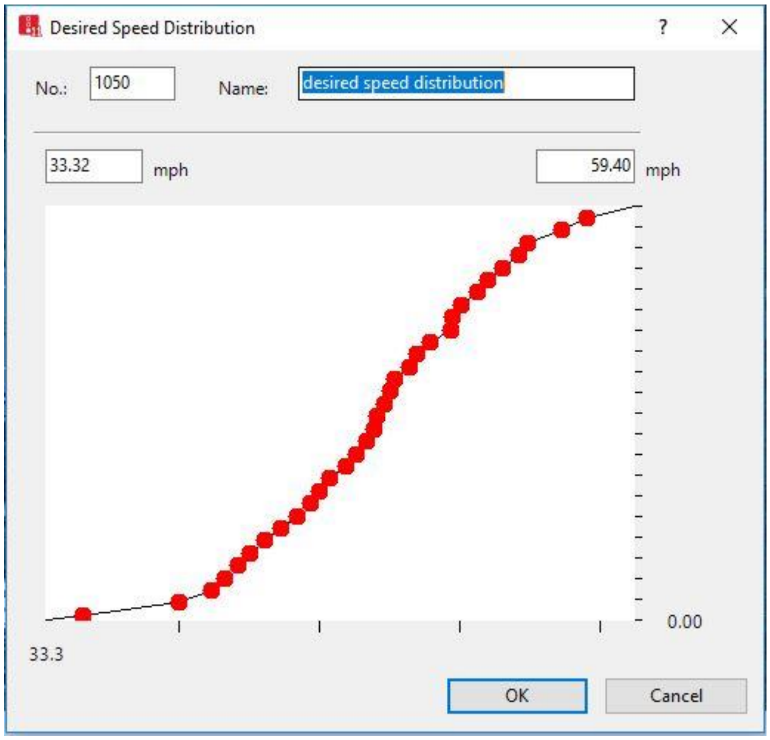

Figure A-3: Desired distribution coded in Vissim.

Coding Route Decision

In this study, static routes were preferred over dynamic assignments since the network was not complex, regardless having five intersections. Since the volume was not uniform throughout the hour, the static route was coded in 15-minute demand increments as recommended in FDOT (2014).

Coding Traffic Demand

Since the network consisted of five intersections, the traffic demand was coded in Vissim for all links entering the network using the vehicle input, following guidelines from PTV (2018). Traffic demand volume input reflected the balanced 15-minute traffic demand volumes as recommended by FDOT (2014). Tables A-2 through A-5, summarize traffic demand volumes.

Table A-2: Balanced 15-Minute Traffic Volumes: First 15-Minute Analysis Period

BALANCED 15-MINUTE TRAFFIC COUNTS (11:00-11:15)												
SW 34TH ST. AND RADIO RD.												
	SBL	SBT	SBR	NBL	NBT	NBR	WBL	WBT	WBR	EBL	EBT	EBR
Demand	10	389			350	21	11		13			
Real Flow	0.025	0.975			0.943	0.057	0.458		0.542			
AV		399			371			24				
SW 34TH ST. AND HULL RD.												
	SBL	SBT	SBR	NBL	NBT	NBR	WBL	WBT	WBR	EBL	EBT	EBR
Demand	42	346	12	12	324	63	48	5	30	17	13	12
Real Flow	0.105	0.865	0.030	0.030	0.812	0.158	0.578	0.060	0.361	0.405	0.310	0.286
AV		400			399			83			42	
SW 34TH ST. AND SW 20TH AVE.												
	SBL	SBT	SBR	NBL	NBT	NBR	WBL	WBT	WBR	EBL	EBT	EBR
Demand	3	343	60	61	289	1	0	1	1	108	0	69
Real Flow	0.007	0.845	0.148	0.174	0.823	0.003	0.000	0.500	0.500	0.610	0.000	0.390
AV		406			351						177	
SW 34TH ST. AND WINDMEADOWS BLVD.												
	SBL	SBT	SBR	NBL	NBT	NBR	WBL	WBT	WBR	EBL	EBT	EBR
Demand	0	345	67	22	288					63		30
Real Flow	0.000	0.837	0.163	0.071	0.929					0.677		0.323
AV		412			310						93	
SW 34TH ST. AND ARCHER RD												
	SBL	SBT	SBR	NBL	NBT	NBR	WBL	WBT	WBR	EBL	EBT	EBR
Demand	86	195	94	119	165	39	45	230	52	98	136	34
Real Flow	0.229	0.520	0.251	0.368	0.511	0.121	0.138	0.703	0.159	0.366	0.507	0.127
AV		375			323			327			268	

Table A-3: Balanced 15-Minute Traffic Volumes: Second 15-Minute Analysis Period

BALANCED 15-MINUTE TRAFFIC COUNTS (11:15-11:30)												
SW 34TH ST. AND RADIO RD.												
	SBL	SBT	SBR	NBL	NBT	NBR	WBL	WBT	WBR	EBL	EBT	EBR
Demand	9	345			352	15	16		15			
Real Flow	0.025	0.975			0.959	0.041	0.516		0.484			
AV		354			367			31				
SW 34TH ST. AND HULL RD.												
	SBL	SBT	SBR	NBL	NBT	NBR	WBL	WBT	WBR	EBL	EBT	EBR
Demand	38	305	18	10	317	64	43	5	24	26	10	10
Real Flow	0.105	0.845	0.050	0.026	0.811	0.164	0.597	0.069	0.333	0.565	0.217	0.217
AV		361			391			72			46	
SW 34TH ST. AND SW 20TH AVE.												
	SBL	SBT	SBR	NBL	NBT	NBR	WBL	WBT	WBR	EBL	EBT	EBR
Demand	1	299	58	53	290	0	0	0	1	101	0	81
Real Flow	0.003	0.835	0.162	0.155	0.845	0.000	0.000	0.000	1.000	0.555	0.000	0.445
AV		358			343						182	
SW 34TH ST. AND WINDMEADOWS BLVD.												
	SBL	SBT	SBR	NBL	NBT	NBR	WBL	WBT	WBR	EBL	EBT	EBR
Demand	0	300	80	27	278					65		30
Real Flow	0.000	0.789	0.211	0.089	0.911					0.684		0.316
AV		380			305						95	
SW 34TH ST. AND ARCHER RD.												
	SBL	SBT	SBR	NBL	NBT	NBR	WBL	WBT	WBR	EBL	EBT	EBR
Demand	80	172	77	111	158	49	40	209	72	77	159	50
Real Flow	0.243	0.523	0.234	0.349	0.497	0.154	0.125	0.651	0.224	0.269	0.556	0.175
AV		329			318			321			286	

Table A-4: Balanced 15-Minute Traffic Volumes: Third 15-Minute Analysis Period

BALANCED 15-MINUTE TRAFFIC COUNTS (11:30-11:45)												
SW 34TH ST. AND RADIO RD.												
	SBL	SBT	SBR	NBL	NBT	NBR	WBL	WBT	WBR	EBL	EBT	EBR
Demand	14	357			368	20	15		13			
Real Flow	0.038	0.962			0.948	0.052	0.536		0.464			
AV		371			388			28				
SW 34TH ST. AND HULL RD.												
	SBL	SBT	SBR	NBL	NBT	NBR	WBL	WBT	WBR	EBL	EBT	EBR
Demand	40	314	17	15	332	67	59	6	31	25	12	9
Real Flow	0.108	0.846	0.046	0.036	0.802	0.162	0.615	0.063	0.323	0.543	0.261	0.196
AV		371			414			96			46	
SW 34TH ST. AND SW 20TH AVE.												
	SBL	SBT	SBR	NBL	NBT	NBR	WBL	WBT	WBR	EBL	EBT	EBR
Demand	1	327	54	68	299	1	0	1	0	114	1	77
Real Flow	0.003	0.856	0.140	0.185	0.812	0.003	0.000	1.000	0.000	0.594	0.005	0.401
AV		382			368						192	
SW 34TH ST. AND WINDMEADOWS BLVD.												
	SBL	SBT	SBR	NBL	NBT	NBR	WBL	WBT	WBR	EBL	EBT	EBR
Demand	2	315	87	15	295					73		32
Real Flow	0.005	0.780	0.215	0.048	0.952					0.695		0.305
AV		404			310						105	
SW 34TH ST. AND ARCHER RD.												
	SBL	SBT	SBR	NBL	NBT	NBR	WBL	WBT	WBR	EBL	EBT	EBR
Demand	82	168	98	117	164	38	44	208	53	97	190	55
Real Flow	0.236	0.483	0.282	0.367	0.514	0.119	0.144	0.682	0.174	0.284	0.556	0.161
AV		348			319			305			342	

Table A-5: Balanced 15-Minute Traffic Volumes: Last 15-Minute Analysis Period

BALANCED 15-MINUTE TRAFFIC COUNTS (11:45-12:00)												
SW 34TH ST. AND RADIO RD.												
	SBL	SBT	SBR	NBL	NBT	NBR	WBL	WBT	WBR	EBL	EBT	EBR
Demand	12	384			359	20	22		16			
Real Flow	0.030	0.970			0.947	0.053	0.579		0.421			
AV		396			379			38				
SW 34TH ST. AND HULL RD.												
	SBL	SBT	SBR	NBL	NBT	NBR	WBL	WBT	WBR	EBL	EBT	EBR
Demand	42	343	21	10	333	68	55	11	23	23	13	10
Real Flow	0.103	0.845	0.052	0.024	0.810	0.165	0.618	0.124	0.258	0.500	0.283	0.217
AV		406			411			89			46	
SW 34TH ST. AND SW 20TH AVE.												
	SBL	SBT	SBR	NBL	NBT	NBR	WBL	WBT	WBR	EBL	EBT	EBR
Demand	2	341	65	69	287	2	0	0	0	124		99
Real Flow	0.005	0.836	0.159	0.193	0.802	0.006	0.000	0.000	0.000	0.556		0.444
AV		408			358						223	
SW 34TH ST. AND WINDMEADOWS BLVD.												
	SBL	SBT	SBR	NBL	NBT	NBR	WBL	WBT	WBR	EBL	EBT	EBR
Demand	1	355	84	23	306					52		36
Real Flow	0.002	0.807	0.191	0.070	0.930					0.591		0.409
AV		440			329						88	
SW 34TH ST. AND ARCHER RD												
	SBL	SBT	SBR	NBL	NBT	NBR	WBL	WBT	WBR	EBL	EBT	EBR
Demand	107	166	118	113	171	43	54	228	51	109	180	61
Real Flow	0.274	0.425	0.302	0.346	0.523	0.131	0.162	0.685	0.153	0.311	0.514	0.174
AV		391			327			333			350	

Coding Traffic Control and Management

Merging Conflict

In Vissim, traffic conflicts caused by merging, diverging, or permissive movements, can be coded using either conflict areas or priority rules. In this study, only traffic conflicts caused by permissive movement within the signalized intersections were considered, and includes conflicts between:

- Right turn-on-red and left turn traffic.
- Right turn-on-red and through traffic from the conflicting movement.
- Unprotected left turn, and the through traffic from the conflicting movement.

Therefore, the aforementioned conflicts were coded using conflict areas and not priority rules, as recommended by FDOT (2014).

Traffic Signal Controller

In Vissim, a traffic signal controller can be built from various sources, including: fixed time, ring barrier controller (RBC), Vehicle Actuating Program (VAP), and importing external signal controller (PTV, 2018). RBC was used in the model to code traffic signal control, and a SYNCHRO model developed by Atkins North America was used to create RBC folders comprised of signal settings, which were then loaded in Vissim (Russo, 2017).

APPENDIX B

Base Model Verification

Software

There were no runtime warnings or errors that affected simulation results, and all RBC errors and warnings were checked and corrected.

Model Run Parameters

Initialization/ warm up period set was checked and confirmed that it was twice the time a vehicle takes to travel the entire network.

Network

Unusual traffic characteristics, especially for lane change restrictions at the intersections and on the links were checked, and link geometries were checked whether they matched the lane schematics.

Demand and Routing

Coded traffic volume and traffic composition was checked and confirmed to be correct. Unusual vehicle routing decision due to connector look back distances was checked and corrected for all right and left turn movements.

Traffic Control

Right turn-on-red and permitted left-turn vehicles were checked if they react properly to the conflict area settings. And all other intersection movements were checked if they react properly to their respective traffic signal head code.

Vehicle Characteristics

Vehicles were checked and ensured there were no lane changes in unrealistic locations, and all the lane changes were done upstream in the appropriate location.

Determining the Required Number of Simulation Runs

In order to replicate the stochasticity of traffic flow, Vissim assigns different random seeds for each run. Random seeding returns different outputs for each run and alters characters, such as when the vehicle enters into the network, which lane to use, the aggressiveness level of the driver, and interaction between vehicles (Radwan et al., 2000).

Vissim does not automatically calculate the required number of runs necessary to achieve good results that are within the tolerable error. Therefore, a preliminary number of runs (10 runs) was assumed, and the required number of runs was calculated using the Equation B-1.

$$n = \left(\frac{s * t_{\frac{\alpha}{2}}}{\mu * \varepsilon}\right)^2 \qquad \text{Equation B-1}$$

Where,

n = required number of simulation runs,

S = standard deviation of the system performance measure based on the previous simulation runs,

$t_{\frac{\alpha}{2}}$ = critical value of a two-sided Student t-statistic at the confidence level of α and n − 1 degrees of freedom (df),

μ = mean of the system performance measure, and

ε = tolerable error, specified as a fraction of μ, desirable value of 10%.

Total traffic volume was used as the MOE for determining the required number of simulation runs, as recommended by FDOT (2014). Based on the preliminary simulation runs, the resulting average total traffic volume was 1228 vph, and the standard deviation was 188 vph. Using Equation B-1, under 95% confidence level, where $t_{.25,9} = 2.262$, and $\varepsilon = 10\%$, the number of runs required was 11.99. Therefore, in this study, twelve (12) simulation runs with different random seeds were enough to produce adequate results.

APPENDIX C

Model Calibration

Traffic Volumes

The results of the comparison between observed traffic volume and its respective simulated link volume, for all segments, are summarized by intersection in Tables C-1 and C-2.

Table C-1: AM Off-Peak Volume Calibration Results for SR 121 from Archer Rd to Radio Rd

ROADWAY	VISSIM LINK NUMBER	LOCATION	OFF PEAK COUNT VOLUME	VISSIM MODEL VOLUME	DIFFERENCE	INDIVIDUAL LINK FLOW				GEH STATISTIC
						<700vph		700vph to 2700vph		
						Within 100vph	Criteria met	Within 15%	Criteria met	
SR 121	78	SR 121 (NB Approach to Windmeadows)	1254	1276	22			1.75%	YES	0.62
	79	SR 121 (NB Approach to Windmeadows)	1254	1276	22			1.75%	YES	0.62
	84	SR 121 (NB Approach to Archer Intersection)	1287	1276	-11			-0.85%	YES	0.31
	85	SR 121 (NB Approach to Archer Intersection)	1287	1276	-11			-0.85%	YES	0.31
	86	SR 121 (SB Approach to Archer Intersection)	1443	1402	-41			-2.84%	YES	1.09
	87	SR 121 (SB Approach to Archer Intersection)	1443	1402	-41			-2.84%	YES	1.09
	80	SR 121 (SB Approach to Windmeadows Intersection)	1636	1584	-52			-3.18%	YES	1.30
	69	SR 121 (NB Approach to 20TH Ave Intersection)	1391	1382	-9			-0.65%	YES	0.24
	10025	SR 121 (NB Approach to 20TH Ave Intersection)	1391	1382	-9			-0.65%	YES	0.24
	70	SR 121 (NB Approach to 20TH Ave Intersection)	1391	1382	-9			-0.65%	YES	0.24
	72	SR 121 (SB Approach to 20TH Ave Intersection)	1586	1532	-54			-3.40%	YES	1.37
	71	SR 121 (SB Approach to 20TH Ave Intersection)	1586	1532	-54			-3.40%	YES	1.37
	59	SR 121 (NB Approach to Hull Intersection)	1615	1543	-72			-4.46%	YES	1.81
	60	SR 121 (NB Approach to Hull Intersection)	1615	1543	-72			-4.46%	YES	1.81
	62	SR 121 (SB Approach to Hull Intersection)	1538	1543	5			0.33%	YES	0.13
	61	SR 121 (SB Approach to Hull Intersection)	1538	1543	5			0.33%	YES	0.13
	53	SR 121 (NB Approach to Radio Intersection)	1505	1488	-17			-1.13%	YES	0.44
	53	SR 121 (SB Approach to Radio Intersection)	1520	1482	-38			-2.50%	YES	0.98
	10019	SR 121 (SB Approach to Radio Intersection)	1520	1482	-38			-2.50%	YES	0.98
	54	SR 121 (SB Approach to Radio Intersection)	1520	1482	-38			-2.50%	YES	0.98

Table C-2: AM Off-Peak Volume Calibration Results for Roads Intersecting SR 121

ROADWAY	VISSIM LINK NUMBER	LOCATION	OFF PEAK COUNT VOLUME	VISSIM MODEL VOLUME	DIFFERENCE	INDIVIDUAL LINK FLOW				GEH STATISTIC
						<700mph		700vph To 2700vph		
						Within 100vph	Criteria Met	Within 15%	Criteria Met	
RADIO RD	56	WB Approach to Radio Intersection	121	118	-3	-3	YES			0.27
	57	WB Approach to Radio Intersection	121	118	-3	-3	YES			0.27
	10020	WB Approach to Radio Intersection	121	118	-3	-3	YES			0.27
HULL RD	63	EB Approach to Hull Intersection	180	176	-4	-4	YES			0.30
	10023	EB Approach to Hull Intersection	180	176	-4	-4	YES			0.30
	64	EB Approach to Hull Intersection	180	176	-4	-4	YES			0.30
	65	WB Approach to Hull Intersection	340	339	-1	-1	YES			0.05
	10024	WB Approach to Hull Intersection	340	339	-1	-1	YES			0.05
	66	WB Approach to Hull Intersection	340	339	-1	-1	YES			0.05
20TH AVE	73	EB Approach to 20TH Intersection	774	778	4			0.52%	YES	0.14
	10027	EB Approach to 20TH Intersection	774	778	4			0.52%	YES	0.14
	74	EB Approach to 20TH Intersection	774	778	4			0.52%	YES	0.14
	75	WB Approach to 20TH Intersection	4	4	0	0	YES			0.00
WINDMEADOWS RD	81	EB Approach to Windmeadows Intersection	381	380	-1	-1	YES			0.05
	10029	EB Approach to Windmeadows Intersection	381	380	-1	-1	YES			0.05
	82	EB Approach to Windmeadows Intersection	381	380	-1	-1	YES			0.05
ARCHER RD	88	EB Approach to Archer Intersection	1246	1230	-16			-1.28%	YES	0.45
	10032	EB Approach to Archer Intersection	1246	1230	-16			-1.28%	YES	0.45
	89	EB Approach to Archer Intersection	1246	1230	-16			-1.28%	YES	0.45
	91	WB Approach to Archer Intersection	1286	1291	5			0.39%	YES	0.14
	10033	WB Approach to Archer Intersection	1286	1291	5			0.39%	YES	0.14
	90	WB Approach to Archer Intersection	1286	1291	5			0.39%	YES	0.14

Note: GEH is an empirical formula expressed as $\sqrt{2 * \frac{(M-C)^2}{M+C}}$ where M is the simulation model volume and C is the field counted volume.

Preliminary Traffic Volume Calibration Results

Based on the results presented in Tables C-1 and C-2, the variation between simulated and measured traffic volumes, for all links with traffic volumes less than 700vph, were within 100vph. This indicates that 100% of the links met the calibration traffic volume target (FDOT, 2014). For all links with traffic volumes of more than 700vph, but less than 2700vph, the variations were within 15%, which means 100% of the links in this category met the calibration traffic volume target. Since no more than 5% variation was present, it was not necessary to check whether the sum of the link volumes within the calibration area were within 5% (FDOT, 2014). Table C-3 summarizes the results of each criteria used for assessing volume calibration.

Table C-3: Traffic Volume Calibration Summary for All Links in the Network

	Off Peak Count	**Simulation**	**Difference**	
Total Traffic Flows For All Links	42308	41748	-560	
Variation For Sum All Link Flows	-1.32%	GEH	2.73	
Sum All Link Flows (FLOWS >85% AND GEH <5)	YES			
Criteria	within <100vph		within 15%	
	NL	MC	NL	MC
Total Count	13	13	29	29
Individual Links	100%		100%	
Individual Links (FLOWS MET FOR >85% CASES AND GEH STATISTIC <5 FOR 85% OF CASES)	YES		YES	

Note: NL = Number of links under specific criteria, MC = Number of links that meet the criteria.

Travel Time

Field measured vehicle travel times were segmented between signalized intersections. The study site had a total of four segments from the beginning of the corridor (Archer Rd and SW 34th St) to the end of the corridor (Radio Rd and SW 34th St). In both directions of each segment, the average vehicle travel time was extracted from the drone video recorded on site, summarized in Tables C-4 and C-5 and graphically represented in Figures C-1 and C-2. Boundaries were established based on the allowable variation of 15%, as recommend by FDOT (2014). These boundaries were then compared with the boundaries that resulted from a single standard deviation from the mean. The greater of two comparisons was taken as the upper boundary, and the lower of the two comparisons was taken as the lower boundary. For similar segments, the resulting simulation travel time was compared, and if the average simulated travel time did not exceed the boundary set, the calibration target was met (FDOT, 2014). All links met the calibration target, for both directions; therefore, the requirement was met that at least 85% of all links meet the travel time calibration target, as indicated in Tables C-4 and C-5.

Table C-4: Calibration Results of Vehicle Travel Times in NB Direction along SR 121

AM-OFF PEAK TRAVEL TIME NB (11:00AM-12:00PM)										
SEGMENT	Distance	Field	15% Range		1 SD		TT Range		Simulation	Threshold
	[mi]	TT[sec]	UB	LB	UB	LB	UB	LB	TT [sec]	
ARCHER-WIND	0.07	10	11	8	12	7	12	7	9.19	YES
WIND-20TH	0.41	38	43	32	39	36	43	32	34.92	YES
20TH-HULL	0.23	26	30	22	27	23	30	22	29.79	YES
HULL-RADIO	0.32	24	27	20	24	23	27	20	26.32	YES

Note: TT = Travel Times, SD = Standard Deviation, UB = Upper Bound, LB = Lower Bound

Table C-5: Calibration Results of Vehicle Travel Times in SB Direction along SR 121

AM OFF-PEAK TRAVEL TIME SB (11:00AM-12:00PM)										
SEGMENT	Distance [mi]	Field TT[sec]	15% Range UB	15% Range LB	1 SD UB	1 SD LB	TT Range UB	TT Range LB	Simulation TT [sec]	Threshold
ARCHER-WIND	0.07	28	33	24	43	14	43	14	29.05	YES
WIND-20TH	0.41	37	42	31	34	34	42	31	41.44	YES
20TH-HULL	0.23	28	32	24	34	22	34	22	27.39	YES
HULL-RADIO	0.32	43	49	36	61	24	61	24	42.56	YES

Note: TT = Travel Times, SD = Standard Deviation, UB = Upper Bound, LB = Lower Bound

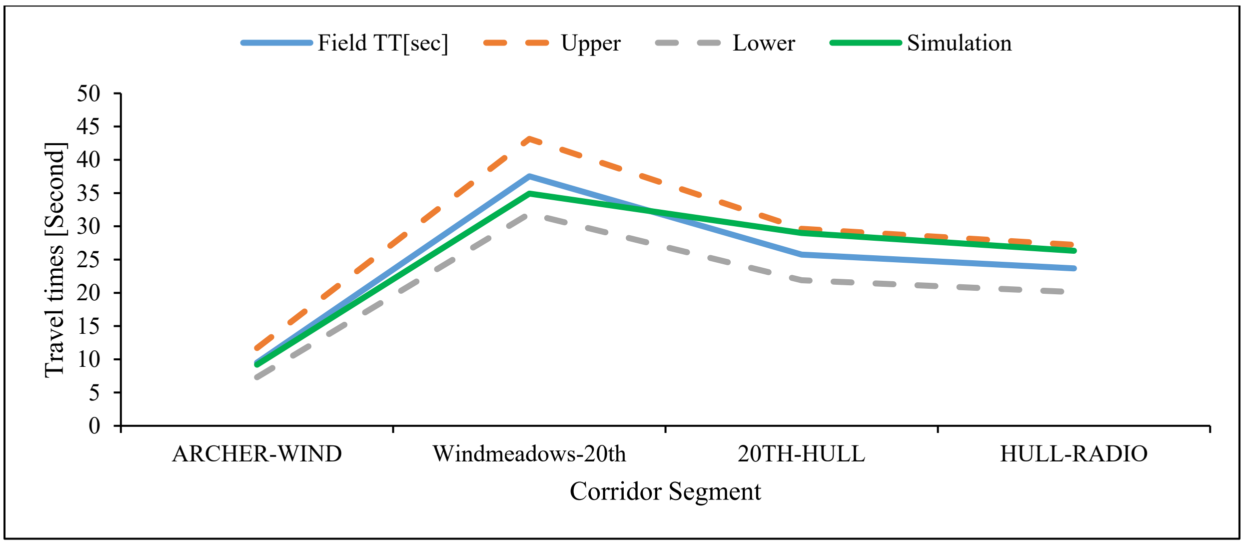

Note: TT = Travel Times.

Figure C-1: Calibration results of travel times in the NB direction along SR 121.

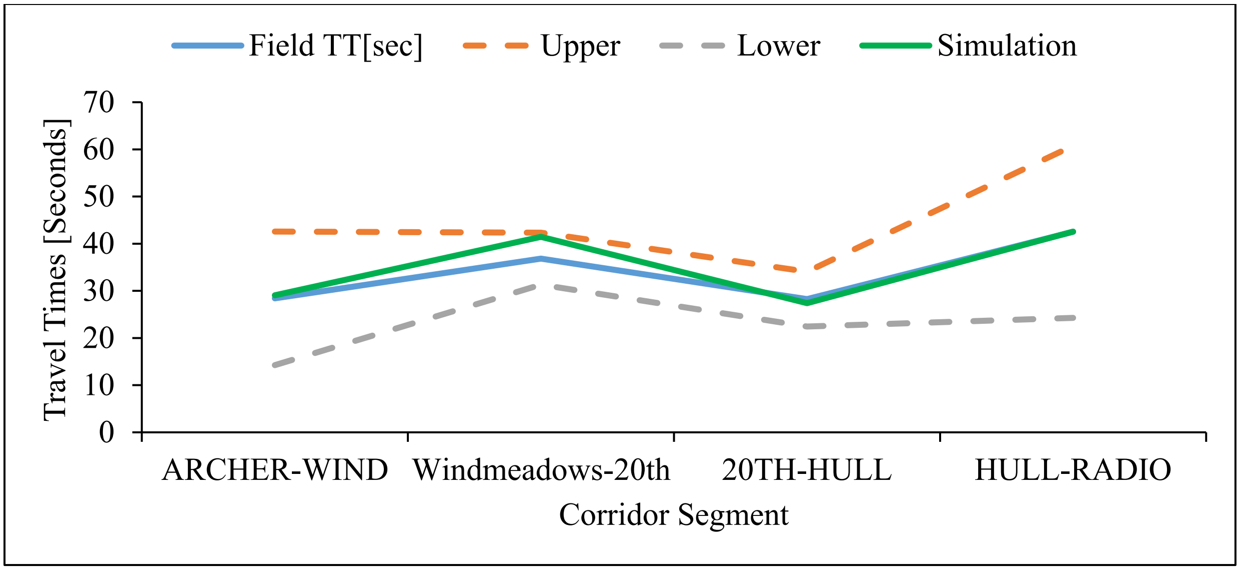

Note: TT = Travel Times.

Figure C-2: Calibration results of travel times in the SB direction along SR 121.

Speed

The calibration target for speed required that an average link speed be within ±10 mph of field measured speeds for at least 85% of all links in the network (FDOT, 2014). Comparison between the simulated results and field measured speeds are summarized in Tables C-6 and C-7, and graphically presented in Figures C-3 and C-4.

Table C-6: Calibration Results of Vehicle Speeds for each Segment along SR 121 NB Direction

AM OFF-PEAK AVERAGE SPEEDS NB				
SEGMENT	Field S[mph]	LB	UB	Simulation
ARCHER-WIND	28	23	36	29
WINDMEADOWS-20TH	39	34	46	42
20TH-HULL	32	28	38	29
HULL-RADIO	49	42	57	44

Note: UB = Upper Bound, LB = Lower Bound

Table C-7: Calibration Results of Vehicle Speeds for Each Segment along SR 121 SB Direction

AM OFF PEAK AVERAGE SPEEDS SB				
SEGMENT	Field S[mph]	LB	UB	Simulation
ARCHER-WIND	9	6	18	9
WINDMEADOWS-20TH	40	35	47	36
20TH-HULL	30	24	37	30
HULL-RADIO	27	19	47	27

Note: UB = Upper Bound, LB = Lower Bound

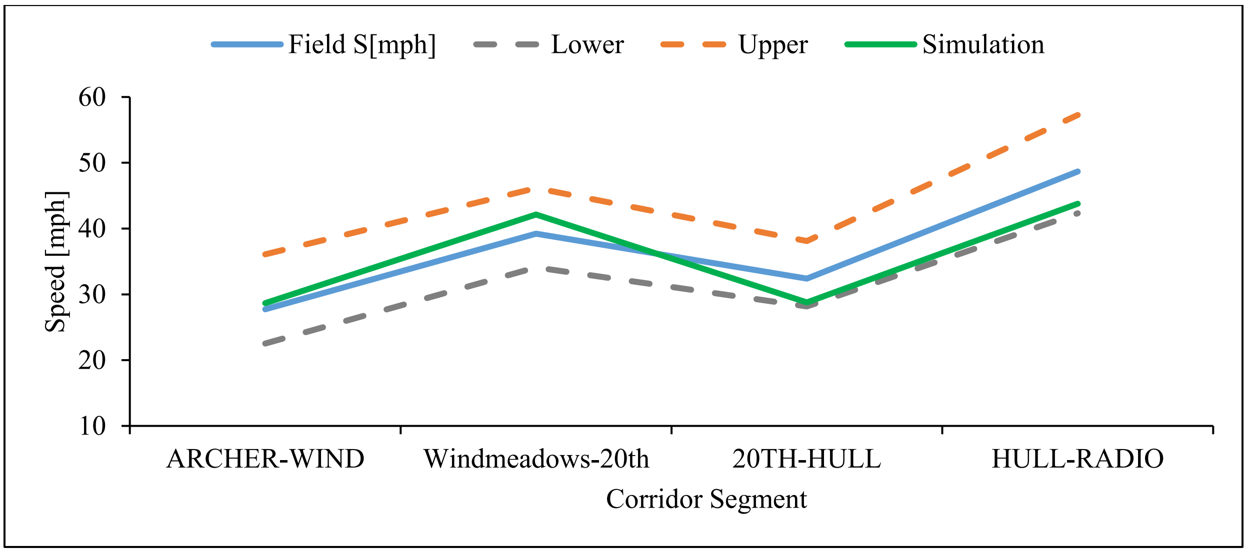

Figure C-3: Calibration results of vehicle speeds for different segments of SR 121 NB direction.

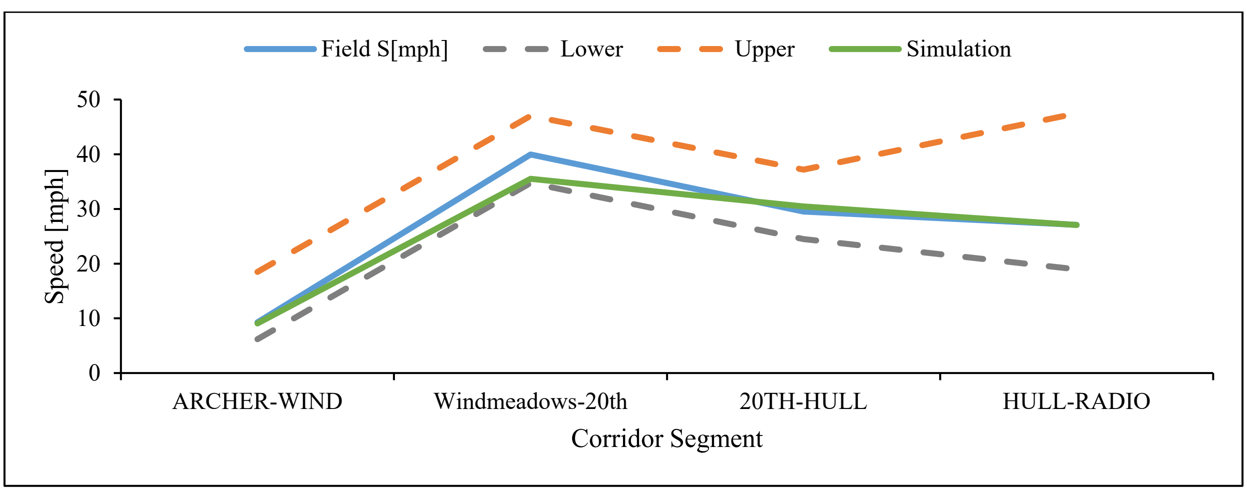

Figure C-4: Calibration results of vehicle speeds for different segments of SR 121 SB direction.

Discharge Headways Calibration

In Vissim, calibration of the discharge headways is conducted by first calibrating the discharge headway of the first queued vehicle, and then calibrating the discharge headways of the remaining queued vehicles. This procedure is followed because the discharge headways calibration of the first position vehicle involves the driver's response to signal changes, while the other discharge headways do not include the driver's response (Saeednia & Menendez, 2017).

Calibration of Discharge Headway of the First Queued Vehicle

In Vissim, the discharge headway of the first queued vehicle is modeled by coding the driver's response to signal changes using either normal reaction time distribution or empirical reaction time distribution. In this study, the empirical distribution was developed from the field measured discharge headways of the first queued vehicle. The empirical reaction time distribution was coded in Vissim per guidelines from PTV (2018).

The calibration process was governed by the calibration target recommended by FDOT (2014). The Root Mean Squared Normalized Error (RMSNE) was used as a goodness-of-fit measure of the discharge headway values between the simulation output and the field data that was used. The values of discharge headways are relatively low, therefore, RMSNE was used for testing the goodness-of-fit because it penalizes large errors heavily (Hollander & Liu, 2008). The fitness function is stated in Equation C-1. An RMSNE of less than 0.15 is considered acceptable for traffic model calibration. The RMSNE calculation for the discharge headways of the first queued vehicle is summarized in Table C-8.

$$\text{RMSNE}=\sqrt{\sum_{i=1}^{n}\frac{1}{n}\left(\frac{(y_{i,sim}-y_{i,field})}{y_{i,sim}}\right)^2} \quad \text{Equation C-1}$$

Where,

$y_{i_{field}}$ = Average field measured discharge headway

$y_{i_{sim}}$ = Average simulated discharge headway for simulation run i

i = number of simulation run

Table C-8: RMSNE Calculation for the Discharge Headways of the First Queued Vehicle

Simulation Run	Average Simulated Result	Average Field Measured Result	$\left(\frac{(y_{i,sim} - y_{i,measured})}{y_{i,sim}}\right)^2$
1	1.15	1.04	0.011
2	1.15	1.04	0.011
3	1.16	1.04	0.013
4	1.15	1.04	0.011
5	1.16	1.04	0.013
6	1.15	1.04	0.011
7	1.16	1.04	0.013
8	1.15	1.04	0.011
9	1.16	1.04	0.013
10	1.15	1.04	0.011
11	1.15	1.04	0.011
12	1.16	1.04	0.013
$\sum\left(\frac{(y_{i,sim} - y_{i,measured})}{y_{i,sim}}\right)^2$			0.1440
N			12
RMSNE= $\sqrt{\sum_{i=1}^{n}\frac{1}{n}\left(\frac{(y_{i,sim}-y_{i,field})}{y_{i,sim}}\right)^2}$			0.110

Calibration of Discharge Headways of the Second to the Tenth Queued Vehicle

In Vissim, starting with the second queued vehicle, discharge headways are greatly influenced by the driving behavior parameters, which is a courtesy of the car-following model. Vissim offers two car-following models: Wiedemann 99 car-following model, recommended for freeways, and Wiedemann 74 car-following model, recommended for arterials (PTV, 2018). In this study, only arterial roads were modeled, therefore, Wiedemann 74 car-following model was used, as shown in Equation C-2.

Calibration of the discharge headways is then completed by adjusting the selected user-adjustable parameters suggested by Byungkyu & Hongtu (2005), Park & Won (2006), Lidbe, Hainen, & Jones (2017, and PTV (2018). The range of values for the user adjustable parameters is shown in Table C-9.

$$\mathrm{d} = \mathrm{a_x} + \mathrm{b_x} \qquad \text{Equation C-2}$$

Where,

d = desired safety distance

$\mathrm{a_x}$ = Stand still distance

$\mathrm{b_x} = (\mathrm{b_{x_{add}}} + \mathrm{b_{x_{mult}}}\ \mathrm{x}\ \mathrm{z})\sqrt{\mathrm{v}}$

$\mathrm{b_{x_{add}}}$ = allows adjustment of the time requirement values

$\mathrm{b_{x_{mult}}}$ = allows adjustment of the standard deviation of the safety distance values

v = vehicle speed

$0 \le \mathrm{z} \ge 1, \mathrm{z} \sim \mathrm{N}(0.5, 0.15^2)$

Table C-9: Wiedemann 74 Car-following Model and Signal Control User-Adjustable Driving Behavior Parameters

	Parameter	**Minimum Value**	**Maximum Value**
Car-following model parameters	Standstill Distance (a_x)	2	8
	Additive part ($b_{x_{add}}$)	0	3
	Multiplicative part ($b_{x_{mult}}$)	0	3
Signal control parameters	Safety distance reduction factor	0	1
	Reaction time distribution	-	-

Initial Evaluation

Before starting the calibration process, an initial simulation was performed, and the resulting average simulated discharge headways of the second to the tenth queued vehicle was compared with the CV and TV field measured discharge headways (see Figure C-5). Regression analysis was performed to evaluate the correlation between the simulated and field discharge headways. Results from the regression analysis are summarized in Table C-10.

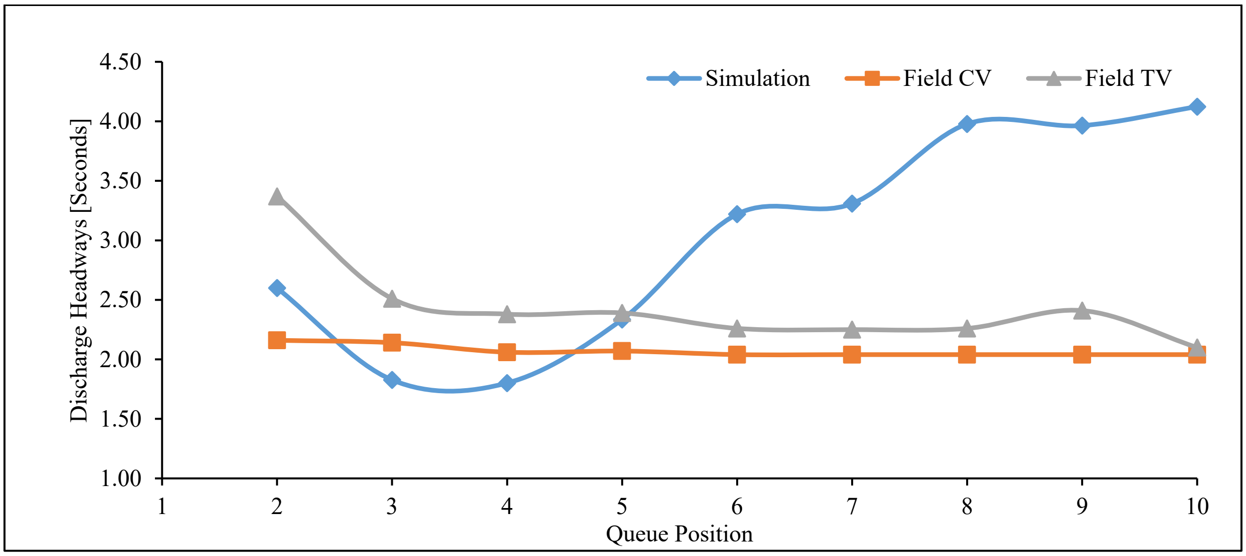

Figure C-5: Comparison of field measured and simulation discharge headways.

Table C-10: Regression Statistic Results Summary of the Initial Evaluation

	Regression Statistics Summary			
	Multiple R	R Square	Adjusted R Square	Standard Error
Simulated and Field CV Discharge Headways	0.623	0.388	-1.286	0.766
Simulated and Field TV Discharge Headways	0.382	0.146	-1.286	0.904

Design of Experiment for calibration of discharge headways starting with 2nd queued vehicle

The factorial design experiment was used to provide all the possible combinations of the control variables that affect the discharge headways while ensuring coverage of the whole parameter surface using MiniTab software. Fractional factorial design (FFD) was performed to omit some of the combinations that would give little or no new information. A total of 16 parameter sets was generated.

Calibration by Using Genetic Algorithm

Many studies used genetic algorithm to simplify the cumbersome task of calibration (Byungkyu & Hongtu, 2005; Lidbe et al., 2017; Ma & Abdulhai, 2001; Manjunatha, Vortisch, & Mathew, 2013). In this study, genetic algorithm was used to provide optimal combinations of parameters that each of them resulted into simulated discharge headways that were close to field measured discharge headways. Therefore, multiple simulation runs were performed based on the provided set of parameters, and the resulting simulated discharge headways were compared with the field measured discharge headways. Genetic Algorithm assigned a fitness value to each of the candidate solutions, and if the stop criterion was not met, a new set of parameters were generated. In this study, the process of selection, single point cross-over, and point mutation, was used to generate the new set of parameters, of which the chances of the previous candidate solutions to appear in the next generation were dependent on the assigned fitness values. Genetic algorithm process is illustrated in Figure C-6.

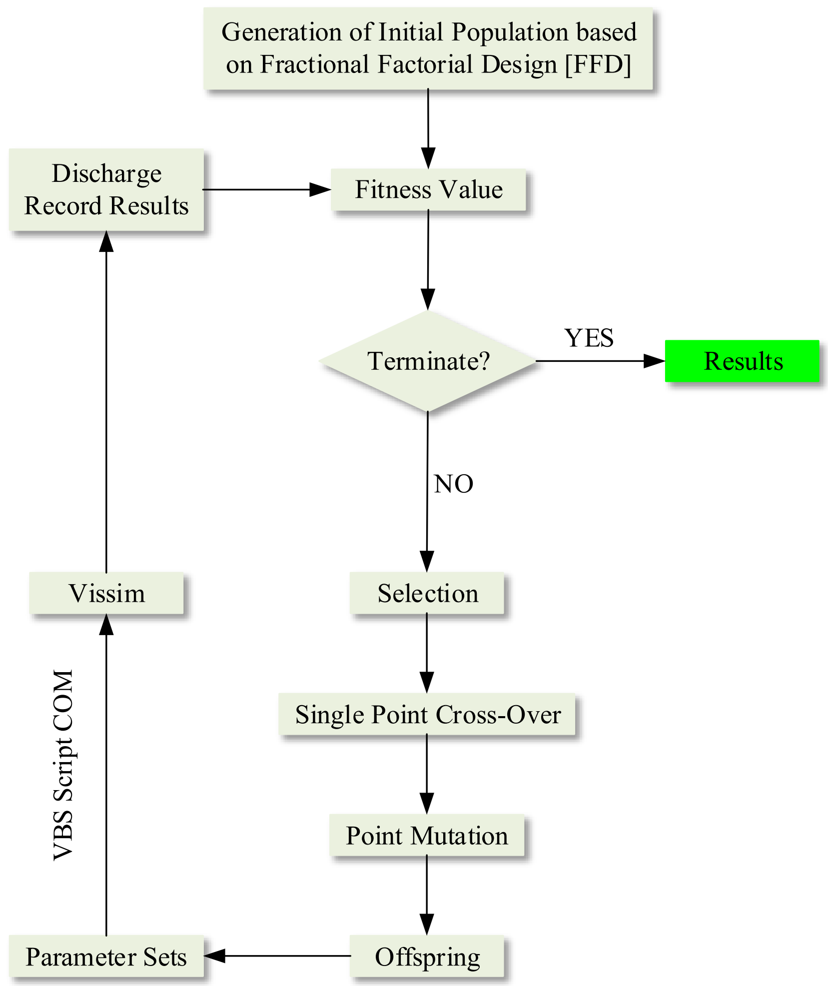

Figure C-6: Genetic Algorithm Flow Chart.

One limitation with calibration discharge headways in Vissim using genetic algorithm is that discharge headway results can only be obtained through direct output files. Therefore, discharge headway results were manually processed before assigning the fitness value for each candidate solution. The visual basic script (VBS) developed was set to enable five simulation runs, with a different random seed for each set of parameters generated by genetic algorithm, in MatLab through the Component Object Model (COM) interface. The resulting discharge headways were manually processed to obtain the average discharge headways of the second through the tenth queued vehicles. For the same reason, the RMSNE was used as a goodness-of-fit measure of the discharge headway values between the simulation output and the field data. A total of 17 and 22 generations with the mutation rate of 5% were evaluated as the algorithm converged for the TV and CV discharge headways, respectively.

Discharge Headways Calibration results

The results of the Vissim calibrated model for both TV and CV traffic conditions are summarized in this section. Figures C-7 and C-8 shows the visual comparison between the resulting discharge headways after calibration and the field measured discharge headways for both TV and CV traffic conditions, respectively. Regression analysis was performed to evaluate the correlation between simulated and field measured discharge headways. The results showed the strongest correlation, with an R-Squared value of 0.93 and 0.89 for both TV and CV traffic conditions, respectively (see Table C-11). The resulting arterial car-following model parameters for TVs only and CVs in mixed traffic, with the suggested values from the FDOT Traffic Analysis Handbook, are summarized in Table C-12.

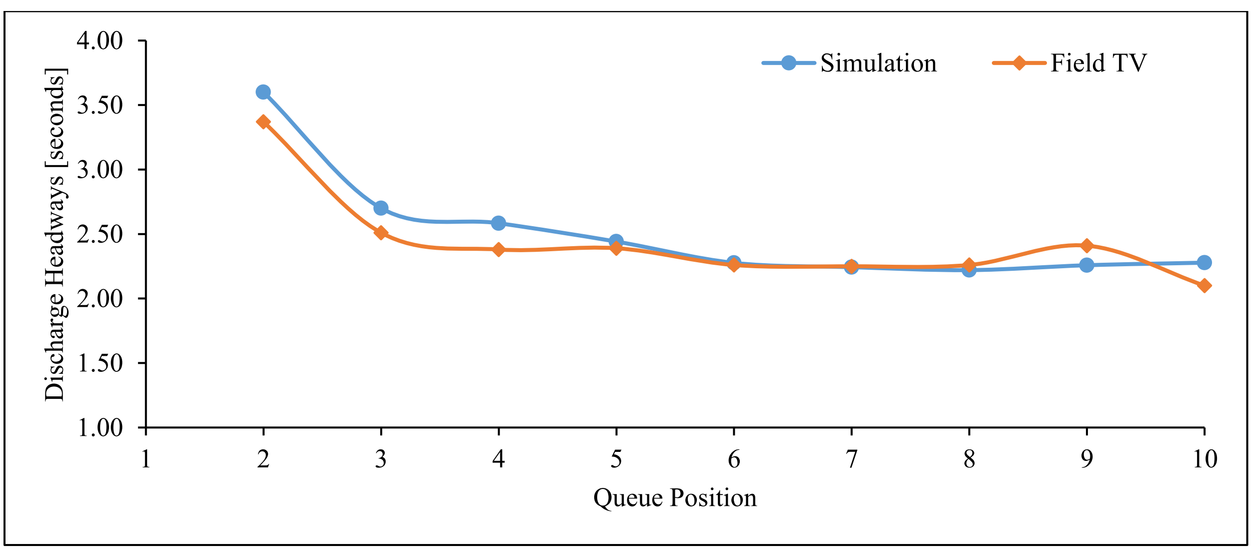

Figure C-7: Comparison of the simulated and field measured TV discharge headways.

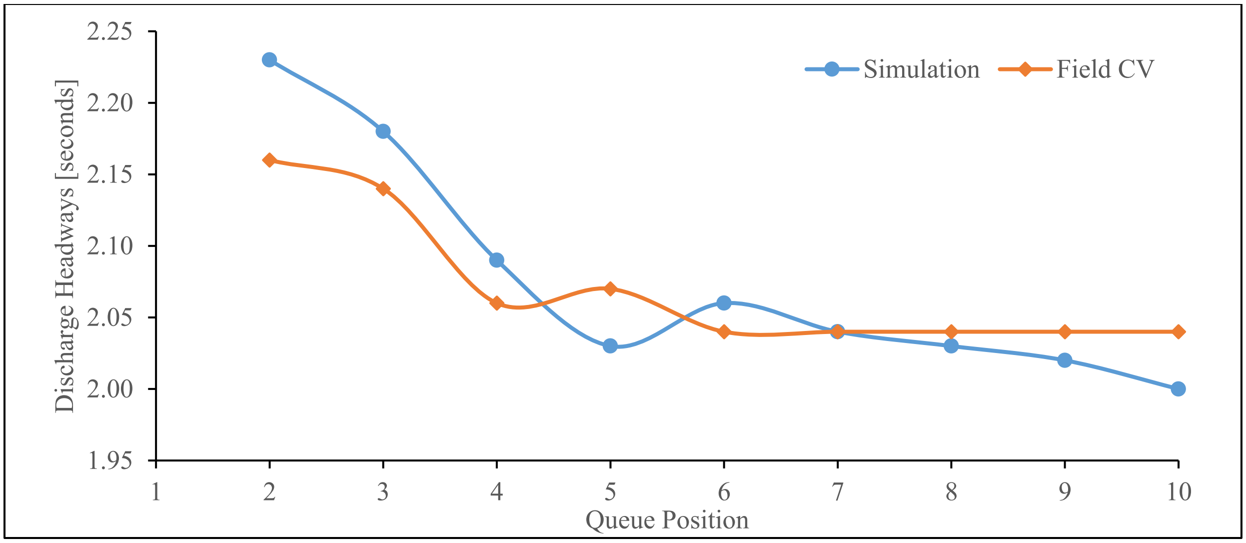

Figure C-8: Comparison of the simulated and field measured CV discharge headways.

Table C-11: Regression Statistic Results Summary after Calibration of the Discharge Headways

	Regression Statistics Summary			
	Multiple R	R Square	Adjusted R Square	Standard Error
Simulated and Field CV Discharge Headways	0.95	0.89	-1.286	0.016
Simulated and Field TV Discharge Headways	0.96	0.92	-1.286	0.128

Table C-12: Arterial Car-Following (Wiedemann 74) Calibrated Parameters and Suggested Range - FDOT Traffic Analysis Handbook

Calibration Parameter	Default Value	Suggested Range	Calibrated value	
			TV	CV in mixed traffic condition
Arterial Car Following (Wiedemann 74)				
Average Standstill distance	6.56 ft	> 3.28 ft	6.56 ft	4.00 ft
Additive part of Safety distance	2.0	1.0 to 3.5	3.0	2.5
Multiplicative part of safety distance	3.00	2.00 to 4.50	4.25	4.30

REFERENCES

Al-Ghamdi, A. S. (1999). Entering Headway for Through Movements at Urban Signalized Intersections. Transportation Research Record: Journal of the Transportation Research Board, 1678(1), 42–47. https://doi.org/10.3141/1678-06

Albertengo, G., Buttazzo, W., Tragno, A., Ricca, M., Torino, P., Bragagnini, A., & Quasso, R. (2014). Smartphone enabled connected vehicles pave the way to intelligent mobility. Proceedings of World Telecommunications Congress (WTC 2014), 1–6.

Alves de Lima, D. (2015). Sensor-based navigation applied to intelligent electric vehicles. University de Technologie Compiegne. Retrieved from https://tel.archives-ouvertes.fr/tel-01213868

Bej, D., Rakshit, S., Mal, A. K., & Mahapatra, R. (2019). A cost-effective system for triggering alarm to distracted drivers/ nurses. Computers & Electrical Engineering, 76, 24–39. https://doi.org/10.1016/J.COMPELECENG.2019.03.001

Bhuiyan, N., Parentela, E., & Inapuri, V. S. (2016). Analysis of Signalized Intersection Crashes. Westernite.org. Westernite.org. Retrieved from https://www.westernite.org/annualmeetings/16_Albuquerque/Papers/9C_Bhuiyan.pdf

Bonneson, J. A. (1992). Study of Headway and Lost Time at Single-Point Urban Interchanges. Transportation Research Board, (1365), 30–39. Retrieved from http://onlinepubs.trb.org/Onlinepubs/trr/1992/1365/1365-004.pdf

Byungkyu, P., & Hongtu, Q. (2005). Development and Evaluation of a Procedure for the Calibration of Simulation Models. Transportation Research Record: Journal of the Transportation Research Board. Transportation Research Board. Retrieved from https://trid.trb.org/view/803577

Calafate, C. T., Cano, J.-C., Manzoni, P., Zaldivar, J., Calafate, C. T., & Cano, J. C. (2011). Providing accident detection in vehicular networks through OBD-II devices and Android-based smartphones. IEEE Workshop on User Mobility and Vehicular Networks, 813–819. https://doi.org/10.1109/LCN.2011.6115556

Cartens, R. L. (1971). Some traffic parameters at signalizations. Traffic Engineering, 41, 33–36.

Connected Signal, Inc. (2018). Crunchbase. Retrieved January 23, 2019, from https://www.crunchbase.com/organization/connected-signals

Cronin, B. (2018). Connected Vehicle Benefits. Retrieved from www.its.dot.gov

Currin, T. R. (2001). Introduction to traffic engineering : a manual for data collection and analysis. Brooks/Cole. Retrieved from https://trid.trb.org/view/678840

Dowling, R., Nevers, B., Jia, A., Skabardonis, A., Krause, C., & Vasudevan, M. (2016). Performance Benefits of Connected Vehicles for Implementing Speed Harmonization. Transportation Research Procedia, 15(ii), 459–470. https://doi.org/10.1016/j.trpro.2016.06.039

El-Den, B. M., Mohamed, M. A., & AbdelFattah, A. I. (2015). Safe Vehicle Driving Using Android Based Smartphones. Advances in Intelligent Systems and Computing, 370, 291–303. https://doi.org/10.1007/978-3-319-21206-7_25

FDOT. (2014). Traffic Analysis Handbook 2014 A Reference for Planning and Operations. Retrieved from http://www.fdot.gov/planning/systems/programs/SM/intjus/pdfs/Traffic Analysis Handbook_March 2014.pdf

FDOT. (2015). Design Exceptions and Design Variations. In Plans Preparation Manual (Vol 1, p. 23). Tallahassee: Florida Department of Transportation.

FDOT. (2017). Florida's Connected and Automated Vehicle Initiative. Florida. Retrieved from http://www.fdot.gov/tr

Greenshields, B. D., Schapiro, D., & Ericksen, E. L. (1946). Traffic Performance at Urban Street Intersections. New Haven. Retrieved from https://trid.trb.org/view/117305

Hollander, Y., & Liu, R. (2008). The principles of calibrating traffic microsimulation models. Transportation, 35(3), 347–362. https://doi.org/10.1007/s11116-007-9156-2

Hurwitz, D. S., Heaslip, K. P., Schrock, S. D., Swake, J., Marnell, P., Tuss, H., & Fitzsimmons, E. (2013). Implications of Distracted Driving on Start-Up Lost Time for Dual Left-Turn Lanes. Journal of Transportation Engineering, 139(9), 923–930. https://doi.org/10.1061/(ASCE)TE.1943-5436.0000569

Islam, M. T., & El-Basyouny, K. (2015). Full Bayesian evaluation of the safety effects of reducing the posted speed limit in urban residential area. Accident Analysis & Prevention, 80, 18–25. https://doi.org/10.1016/j.aap.2015.02.026

Jadaan, K., Zeater, S., & Abukhalil, Y. (2017). Connected Vehicles: An Innovative Transport Technology. Procedia Engineering, 187, 641–648. https://doi.org/10.1016/J.PROENG.2017.04.425

Jin, X., Zhang, Y., Wang, F., Li, L., Yao, D., Su, Y., & Wei, Z. (2009). Departure headways at signalized intersections: A log-normal distribution model approach. Transportation Research Part C: Emerging Technologies, 17(3), 318–327. https://doi.org/10.1016/J.TRC.2009.01.003

Krcal, J., Nagy, I., & Jerabek, M. (2009). Mathematical application for departure model. In Proceedings of the 2009 Euro American Conference on Telematics and Information Systems New Opportunities to increase Digital Citizenship - EATIS '09 (pp. 1–4). New York, New York, USA: ACM Press. https://doi.org/10.1145/1551722.1551750

Lee, C., Saccomanno, F., & Hellinga, B. (2002). Analysis of Crash Precursors on Instrumented Freeways. Transportation Research Record: Journal of the Transportation Research Board, 1784(1), 1–8. https://doi.org/10.3141/1784-01

Lee, J., & Chen, R. L. (1986). Entering Headway at Signalized Intersections in a Small Metropolitan Area. Transportation Research Record, National Research Council, 117–126.

Lee, J., & Park, B. B. (2013). Evaluation of Variable Speed Limit under Connected Vehicle environment. In 2013 International Conference on Connected Vehicles and Expo (ICCVE) (pp. 966–967). IEEE. https://doi.org/10.1109/ICCVE.2013.6799944

Li, H., & Prevedouros, P. D. (2002). Detailed Observations of Saturation Headways and Start-Up Lost Times. Transportation Research Record: Journal of the Transportation Research Board, 1802(1), 44–53. https://doi.org/10.3141/1802-06

Li, T., & Kockelman, K. M. (2016). Valuing the Benefits of Connected and Automated Vehicle Technologies. Transportation Research Board 95th Annual Meeting, 22. Retrieved from https://www.caee.utexas.edu/prof/kockelman/public_html/trb16cavsafety.pdf

Li, X., Oviedo-Trespalacios, O., Rakotonirainy, A., & Yan, X. (2019). Collision risk management of cognitively distracted drivers in a car-following situation. Transportation Research Part F: Traffic Psychology and Behaviour, 60, 288–298. https://doi.org/10.1016/J.TRF.2018.10.011

Lidbe, A. D., Hainen, A. M., & Jones, S. L. (2017). Comparative study of simulated annealing, tabu search, and the genetic algorithm for calibration of the microsimulation model. Simulation, 93(1), 21–33. https://doi.org/10.1177/0037549716683028

Limanond, T., Prabjabok, P., & Tippayawong, K. (2010). Exploring impacts of countdown timers on traffic operations and driver behavior at a signalized intersection in Bangkok. Transport Policy, 17(6), 420–427. https://doi.org/10.1016/j.tranpol.2010.04.009

Liu, P., Yu, H., Wang, W., Ma, J., & Wang, S. (2012). Evaluating the Effects of Signal Countdown Timers on Queue Discharge Characteristics at Signalized Intersections in China. Transportation Research Record: Journal of the Transportation Research Board, 2286(1), 39–48. https://doi.org/10.3141/2286-05

Ma, T., & Abdulhai, B. (2001). Genetic algorithm-based combinatorial parametric optimization for the calibration of microscopic traffic simulation models. ITSC 2001. 2001 IEEE Intelligent Transportation Systems. Proceedings (Cat. No.01TH8585), 848–853. https://doi.org/10.1109/ITSC.2001.948771

Manjunatha, P., Vortisch, P., & Mathew, T. (2013). Methodology for the Calibration of VISSIM in Mixed Traffic. Transportation Research Board 92nd Annual Meeting, 11.

Mannering, F. L., & Washburn, S. S. (2014). Principles of highway engineering and traffic analysis. Retrieved from https://books.google.com/books?id=8DBuDwAAQBAJ&printsec=frontcover&dq=principles+of+highway+engineering+and+traffic+analysis&hl=en&sa=X&ved=0ahUKEwjMv4TkqMPfAhUPA6wKHTA_CyIQ6AEIKjAA#v=onepage&q=principles of highway engineering and traffic analysis&f=fals

McClave, J. T., & Sincich, T. (2009). Statistics (11th ed.). Florida: Pearson Education.

Motamedidehkordi, N., Margreiter, M., & Benz, T. (2016). Shockwave Suppression by Vehicle-to-Vehicle Communication. Transportation Research Procedia, 15, 471–482. https://doi.org/10.1016/j.trpro.2016.06.040

Najm, W. G., Smith, J. D., & Yanagisawa, M. (2007). Pre-Crash Scenario Typology for Crash Avoidance Research. Washington D.C. Retrieved from https://www.nhtsa.gov/sites/nhtsa.dot.gov/files/pre-crash_scenario_typology-final_pdf_version_5-2-07.pdf

National Research Council (U.S.). Transportation Research Board. (2010). Highway Capacity Manual. (5th ed.). Washington, D.C. : Transportation Research Board.

Neto, G. L. D. C., De Lima, D. A., & Neto, A. D. M. (2016). The Use of Smartphones as a Smart Sensor for Intelligent Vehicles. Proceedings - 13th Latin American Robotics Symposium and 4th Brazilian Symposium on Robotics, LARS/SBR 2016, 37–42. https://doi.org/10.1109/LARS-SBR.2016.14

Njobelo, G., Sando, T., Sajjadi, S., Mtoi, E., Ozguven, E. E., & Sobanjo, J. (2018). Safety Evaluation of the Advanced Stop Assist System in Connected Vehicle Environment. Transportation Research Record: Journal of the Transportation Research Board, 2672(22), 47–57. https://doi.org/10.1177/0361198118797831

Oviedo-Trespalacios, O., King, M., Haque, M. M., & Washington, S. (2017). Risk factors of mobile phone use while driving in Queensland: Prevalence, attitudes, crash risk perception, and task-management strategies. PLOS ONE, 12(9), e0183361. https://doi.org/10.1371/journal.pone.0183361

Park, B. (Brian), & Won, J. (2006). Microscopic Simulation Model Calibration and Validation Handbook. Transportation Research Board, 174. Retrieved from https://trid.trb.org/view/798078

PTV. (2018). PTV VISSIM 11 User Manual. Karlsruhe, Germany: PTV GROUP.

Radwan, E., Shankar Ramasamy, P., Harb, R., Russo, C., Zarillo, M., & Gordin, E. (2000). Calibration and Validation of Shaker and TNCC for deployment on Florida's turnpike. Journal of Transportation Engineering, 136, 85–92. Retrieved from https://doi.org/10.1061/(ASCE)TE.1943 5436.0000060.

Ramezani, H., & Benekohal, R. (2015). Optimized Speed Harmonization with Connected

Vehicles for Work Zones. IEEE Conference on Intelligent Transportation Systems, Proceedings, ITSC, 2015–Octob, 1081–1086. https://doi.org/10.1109/ITSC.2015.179

RITA. (2010). ITS Joint Program Office Research and nnovative Technology Administration (RITA). Achieving the Vision: From VII to IntellDrive.

Russo, C. (2017). Signal Retiming Report Study (Vol. 121). Orlando.

Saeednia, M., & Menendez, M. (2017). A consensus-based algorithm for truck platooning. IEEE Transactions on Intelligent Transportation Systems, 18(2), 404–415. https://doi.org/10.1109/TITS.2016.2579260

Sayed, T., & Sacchi, E. (2016). Evaluating the safety impact of increased speed limits on rural highways in British Columbia. Accident Analysis & Prevention, 95, 172–177. https://doi.org/10.1016/J.AAP.2016.07.012

Schakel, W. J., & van Arem, B. (2014). Improving Traffic Flow Efficiency by In-Car Advice on Lane, Speed, and Headway. IEEE Transactions on Intelligent Transportation Systems, 15(4), 1597–1606. https://doi.org/10.1109/TITS.2014.2303577

Schakel, W. J., & Van Arem, B. (2014). Improving traffic flow efficiency by in-car advice on lane, speed, and Headway. IEEE Transactions on Intelligent Transportation Systems, 15(4), 1597–1606. https://doi.org/10.1109/TITS.2014.2303577

Sharma, A., Vanajakshi, L., & Rao, N. (2009). Effect of Phase Countdown Timers on Queue Discharge Characteristics under Heterogeneous Traffic Conditions. Transportation Research Record: Journal of the Transportation Research Board, 2130(1), 93–100. https://doi.org/10.3141/2130-12

Shawky, M., & Al-ghafli, A. (2016). Start-up delay Estimation at Signalized Intersections : Impact of Left-Turn Phasing Sequences. International Journal of Engineering and Applied Sciences, 3(11), 7–12.

Soualmi, B., Sentouh, C., Popieul, J. C., & Debernard, S. (2014). Automation-driver cooperative driving in presence of undetected obstacles. Control Engineering Practice, 24, 106–119. https://doi.org/10.1016/j.conengprac.2013.11.015

Stebbins, S., Hickman, M., Kim, J., & Vu, H. L. (2017). Characterising Green Light Optimal Speed Advisory trajectories for platoon-based optimisation. Transportation Research Part C: Emerging Technologies, 82, 43–62. https://doi.org/10.1016/J.TRC.2017.06.014

Stephens, D., Schroeder, J., Klein, R., & Institute, B. M. (2015, August 1). Vehicle-to-infrastructure (V2I) safety applications performance requirements, vol. 3, red light violation warning (RLVW). United States. Department of Transportation. Intelligent Transportation Systems Joint Program Office. Retrieved from https://rosap.ntl.bts.gov/view/dot/32029

Stevanovic, A., Stevanovic, J., & Kergaye, C. (2013). Green Light Optimized Speed Advisory Systems. Transportation Research Record: Journal of the Transportation Research Board, 2390(1), 53–59. https://doi.org/10.3141/2390-06

Talebpour, A., Mahmassani, H., & Hamdar, S. (2013). Speed Harmonization. Transportation Research Record: Journal of the Transportation Research Board, 2391, 69–79. https://doi.org/10.3141/2391-07

Tan, J., Li, L., Li, Z., & Zhang, Y. (2013). Distribution models for start-up lost time and effective departure flow rate. Transportation Research Part A: Policy and Practice, 51, 1–11. https://doi.org/10.1016/j.tra.2013.03.001

U.S. Department of Transportation. (2017). Connected Vehicle-Safety ITS Benefits, Costs, and Lessons Learned. Retrieved from www.its.dot.gov

Waller, S., Ng, M., Ferguson, E., Nezamuddin, N., & Sun, D. (2009). Speed Harmonization and Peak-period Shoulder Use to Manage Urban Freeway Congestion, 7. Retrieved from http://trid.trb.org/view.aspx?id=919215

Yang, S. (2013). Enlarged stopping distance to improve vehicle discharge at urban signalised intersections. Queensland University of Technology. Retrieved from https://eprints.qut.edu.au/60871/1/Shuai_Yang_Thesis.pdf

Yin, S., Su, Y., Wang, C., Yao, D., Li, L., & Zhang, Y. (2011). Comparison of Vehicle Departure Headways in Beijing and Atlanta. Tsinghua Science & Technology, 16(3), 332–336. https://doi.org/10.1016/S1007-0214(11)70048-7

Zhang, G., Wang, Y., Wei, H., & Chen, Y. (2007). Examining Headway Distribution Models Using Urban Freeway Loop Event Data. Transportation Research Journal, 1999, 141–149. https://doi.org/10.3141/1999-15

VITA

EDUCATION

Master of Science in Civil Engineering, April, 2019 University of North Florida	Jacksonville, Florida
Bachelor of Science in Civil Engineering, July, 2016 University of Dar es Salaam	Dar es Salaam, Tanzania

PROFESSIONAL EXPERIENCE

University of North Florida, Jacksonville, Florida Graduate Research Assistant	August 2017- April 2019
Arcadis U.S., Inc. Jacksonville Office, Florida Transportation/Traffic Technical Intern	February 2019 – April 2019
Tanzania Road Agency, Dar-es Salaam, Tanzania Transportation Engineer	November 2016 – June 2017